

1 **Impact of dust addition on the microbial food web under present and future**
2 **conditions of pH and temperature**

3

4 Julie Dinasquet^{1,2*}, Estelle Bigeard³, Frédéric Gazeau⁴, Farooq Azam¹, Cécile Guieu⁴, Emilio
5 Marañón⁵, Céline Ridame⁶, France Van Wambeke⁷, Ingrid Obernosterer² and Anne-Claire
6 Baudoux³

7 ¹ Marine Biology Research Division, Scripps Institution of Oceanography, UCSD, USA

8 ² Sorbonne Université, CNRS, Laboratoire d'Océanographie Microbienne, LOMIC, France

9 ³ Sorbonne Université, CNRS, Station Biologique de Roscoff, UMR 7144 Adaptation et
10 Diversité en Milieu Marin, France

11 ⁴ Sorbonne Université, CNRS, Laboratoire d'Océanographie de Villefranche, LOV, 06230
12 Villefranche-sur-Mer, France

13 ⁵ Department of Ecology and Animal Biology, Universidade de Vigo, Spain

14 ⁶ CNRS-INSU/IRD/MNHN/UPMC, LOCEAN: Laboratoire d'Océanographie et du Climat:
15 Expérimentation et Approches Numériques, UMR 7159

16 ⁷ Aix-Marseille Université, CNRS/INSU, Université de Toulon, IRD, Mediterranean Institute of
17 Oceanography, UM110, France

18 *Corresponding: jdinasquet@ucsd.edu, present address: Center for Aerosol Impact on Chemistry
19 of the Environment (CAICE), Scripps Institution of Oceanography, UCSD, USA

20 **Keywords:** bacteria, microeukaryotes, virus, community composition, top-down

21 **Abstract**

22 In the oligotrophic waters of the Mediterranean Sea, during the stratification period, the
23 microbial loop relies on pulsed inputs of nutrients through atmospheric deposition of aerosols
24 from both natural (*e.g.* Saharan dust), anthropogenic or mixed origins. While the influence of
25 dust deposition on microbial processes and community composition is still not fully constrained,
26 the extent to which future environmental conditions will affect dust inputs and the microbial
27 response is not known. The impact of atmospheric wet dust deposition was studied both under
28 present and future environmental conditions (+3°C warming and acidification of -0.3 pH units),
29 through experiments in 300 L climate reactors. Three Saharan dust addition experiments were
30 performed with surface seawater collected from the Tyrrhenian Sea, Ionian Sea and Algerian
31 basin in the Western Mediterranean Sea during the PEACETIME cruise in May-June 2017. Top-
32 down controls on bacteria, viral processes, and community, as well as microbial community
33 structure (16S and 18S rDNA amplicon sequencing) were followed over the 3-4 days
34 experiments. Different microbial and viral responses to dust were observed rapidly after addition
35 and were most of the time more pronounced when combined to future environmental conditions.
36 The dust input of nutrients and trace metals changed the microbial ecosystem from bottom-up
37 limited to a top-down controlled bacterial community, likely from grazing and induced lysogeny.
38 The relative abundance of mixotrophic microeukaryotes and phototrophic prokaryotes also
39 increased. Overall, these results suggest that the effect of dust deposition on the microbial loop is
40 dependent on the initial microbial assemblage and metabolic state of the tested water, and that
41 predicted warming, and acidification will intensify these responses, affecting food web processes
42 and biogeochemical cycles.

43 1. Introduction

44 Input of essential nutrients and trace metals through aerosol deposition is crucial to the ocean
45 surface water biogeochemistry and productivity (at the global scale: *e.g.*, Mahowald et al., 2017;
46 in the Mediterranean Sea: *e.g.*, Guieu and Ridame, 2020) with episodic fertilization events
47 driving microbial processes in oligotrophic regions such as the Pacific Ocean, the Southern
48 Ocean and the Mediterranean Sea.

49 The summer Mediterranean food web is characterized by low primary production (PP) and
50 heterotrophic prokaryotic production (more classically abbreviated as BP for bacterial
51 production) constrained by nutrient availability. Low BP further limits dissolved organic matter
52 (DOM) utilization and export, resulting in DOM accumulation. Therefore, inputs of bioavailable
53 nutrients through deposition of atmospheric particles are essential to the Mediterranean Sea
54 microbial ecosystem. Indeed, these nutrient pulses have been shown to support microbial
55 processes but the extent to which the microbial food web is affected might be dependent on the
56 degree of oligotrophy of the water (Marín-Beltrán et al., 2019; Marañón et al., 2010).

57 In the Mediterranean Sea, dust deposition may stimulates PP and N₂ fixation (Guieu et al.,
58 2014; Ridame et al., 2011, 2021) but also BP, bacterial respiration, virus production, grazing
59 activities, and can alter the composition of the microbial community (*e.g.*, Pulido-Villena et al.,
60 2014; Tsiola et al., 2017; Guo et al., 2016; Pitta et al., 2017; Marín-Beltrán et al., 2019). Overall,
61 in such oligotrophic system, dust deposition appears to predominantly promote heterotrophic
62 activity which will increase respiration rates and CO₂ release.

63 Anthropogenic CO₂ emissions are projected to induce an increase in seawater temperature
64 and an accumulation of CO₂ in the ocean, leading to its acidification and an alteration of ocean
65 carbonate chemistry (IPCC, 2014). In response to ocean warming and increased stratification,

66 low nutrient low chlorophyll (LNLC) regions such as the Mediterranean Sea, are projected to
67 expand in the future (Durrieu de Madron et al., 2011). Moreover, dust deposition is also expected
68 to increase due to desertification (Moulin and Chiapello, 2006). For these reasons, in the future
69 ocean, the microbial food web might become even more dependent on atmospheric deposition of
70 nutrients. Expected increased temperature and acidification might have complex effects on the
71 microbial loop by modifying microbial and viral and community (*e.g.*, Highfield et al., 2017;
72 Krause et al., 2012; Hu et al., 2021; Allen et al., 2020; Malits et al., 2021). While increasing
73 temperature in combination with nutrient input might enhance heterotrophic bacterial growth
74 (Degerman et al., 2012; Morán et al., 2020) more than PP (Marañón et al., 2018), future
75 environmental conditions could push even further this microbial community towards
76 heterotrophy. But so far, the role of dust on the microbial food web in future climate scenarios is
77 unknown.

78 Here, we studied the response of Mediterranean microbial and viral communities (*i.e.*, viral
79 strategies, microbial growth and controls, as well as community composition) to simulated wet
80 Saharan dust deposition during onboard minicosm experiments conducted in three different
81 basins of the Western and Central Mediterranean Sea under present and future projected
82 conditions of temperature and pH. To our knowledge, this is the first study assessing the effect of
83 atmospheric deposition on the microbial food web under future environmental conditions.

84 2. Material & Method

85 *2.1 Experimental set-up*

86 During the ‘ProcEss studies at the Air-sEa Interface after dust deposition in the
87 MEDiterranean sea’ project cruise (PEACETIME), onboard the R/V “Pourquoi Pas ?” in
88 May/June 2017, three experiments were conducted in 300 L climate reactors (minicosms) filled
89 with surface seawater collected at three different stations (Table 1), in the Tyrrhenian Sea (TYR),
90 Ionian Sea (ION) and in the Algerian basin (FAST). The experimental set-up is described in
91 details in Gazeau et al. (2021a). Briefly, the experiments were conducted for 3 days (TYR and
92 ION) and 4 days (FAST) in trace metal free conditions, under light, temperature and pH-
93 controlled conditions following ambient or future projected conditions of temperature and pH.
94 For each experiment, the biogeochemical evolution of the water, after dust deposition, under
95 present and future environmental conditions was followed in three duplicate treatments: i)
96 CONTROL (C1, C2) with no dust addition and under present pH and temperature conditions, ii)
97 DUST (D1, D2) with dust addition under present environmental conditions and iii)
98 GREENHOUSE (G1, G2) with dust addition under projected temperature and pH for 2100
99 (IPCC, 2014; ca. +3 °C and -0.3 pH units). Water was acidified by addition of CO₂ saturated 0.2
100 µm filtered seawater and slowly warmed overnight (Gazeau et al, 2021a). The same dust analog
101 was used as during the DUNE 2009 experiments as described in Desboeufs et al. (2014) and the
102 same dust wet flux of 10 g m⁻² was simulated (as described in Gazeau et al 2021a). Briefly, the
103 dust was derived from the <20 µm fraction of soil collected in Southern Tunisia (a major source
104 for material transported and deposited in the Northwestern Mediterranean) with most particles
105 (99%) smaller than 0.1 µm (Desboeufs et al., 2014). The collected material underwent an
106 artificial chemical aging process by addition of nitric and sulfuric acid (HNO₃ and H₂SO₄,

107 respectively) to mimic cloud processes during atmospheric transport of aerosol with
108 anthropogenic acid gases (Guieu et al., 2010, and references therein). To mimic a realistic wet
109 flux event for the Mediterranean of 10 g m^{-2} , 3.6 g of this analog dust were quickly diluted in 2 L
110 ultrahigh-purity, and sprayed at the surface of the dust amended treatments (D1, D2 and G1, G2;
111 Gazeau et al., 2021a). Such deposition event represents a high but realistic scenario, as several
112 studies reported even higher short wet deposition events in this area of the Mediterranean Sea
113 (Ternon et al., 2010; Bonnet and Guieu, 2006; Loÿe-Pilot and Martin, 1996), suggesting that wet
114 deposition is the main pathway of dust input in the Western Mediterranean Sea.

115 Samples for all parameters (except described below) were taken at t-12h (while filling the
116 tanks), t0 (just before dust addition), t1h, t6h, t12h, t24h, t48h, t72h and t96h (after dust addition,
117 and t96h only for FAST).

118 2.2. Growth rates, mortality, and top down controls

119 BP was estimated at all sampling points from rates of ^3H -Leucine incorporation
120 (Kirchman et al., 1985; Smith and Azam, 1992) as described in Gazeau et al. (2021b). Briefly,
121 triplicate 1.5 mL samples and one blank were incubated in the dark for 1-2 h after addition of 20
122 nM of a mix of cold and ^3H -leucine in two temperature-controlled incubators maintained
123 respectively at ambient temperature for C1, C2, D1 and D2 and at ambient temperature +3 °C for
124 G1 and G2. Heterotrophic prokaryotes (HB) and heterotrophic nanoflagellates (HNF) abundances
125 were measured by flow cytometry as described in Gazeau et al. (2021a). Briefly, samples (4.5
126 mL) were fixed with glutaraldehyde grade I (1% final concentration) and stored at -80°C until
127 analysis. Counts were performed on a FACSCanto II flow cytometer (Becton Dickinson©). Cells
128 were stained with SYBR Green I at 0.025% (vol / vol) final concentration (Gasol & DelGiorgio
129 2000, Christaki et al 2011). Bacterial biomass specific growth rates (BBGR) were estimated

130 following Kirchman (2002), BP/Bacterial Biomass, assuming a carbon to cell ration of 20 fg C
131 cell⁻¹ (Lee and Fuhrman, 1987). Mortality was estimated as the difference between HB present
132 between two successive sampling points and those produced during that time.

133 2.3. Viral abundance, production and life strategy

134 Virus abundances were determined on glutaraldehyde fixed samples (0.5% final
135 concentration, Grade II, Sigma Aldrich, St Louis, MO, USA) stored at -80 °C until analysis. Flow
136 cytometry analysis was performed as described by Brussaard (2004). Briefly, samples were
137 thawed at 37 °C, diluted in 0.2 µm filtered autoclaved TE buffer (10:1 Tris-EDTA, pH 8) and
138 stained with SYBR-Green I (0.5 × 10⁻⁴ of the commercial stock, Life Technologies, Saint-Aubin,
139 France) for 10 min at 80 °C. Virus particles were discriminated based on their green fluorescence
140 and SSC during 1 min analyses (Fig. S1). All cytogram analyses were performed with the Flowing
141 Software freeware (Turku Center of Biotechnology, Finland).

142 Viral production and bacterial losses due to phages were assessed by the virus reduction approach
143 (Weinbauer et al., 2010) at t0 and t24 h in all six minicosms. Briefly, 3 L of seawater were-filtered
144 through 1.2-µm-pore-size polycarbonate filter (Whatman©), and HB (filtrate) were concentrated
145 by ultrafiltration (0.22 µm pore size, Vivaflow 200© polyethersulfone, PES) down to a volume of
146 50 mL. Virus-free water was obtained by filtering 1 L of seawater through a 30 kDa pore-size
147 cartridge (Vivaflow 200©, PES). Six mixtures of HB concentrate (2 mL) diluted in virus-free water
148 (23 mL) were prepared and distributed into 50 mL Falcon tubes. Three of the tubes were incubated
149 as controls, while the other three were inoculated with mitomycin C (Sigma-Aldrich, 1 µg mL⁻¹
150 final concentration) as inducing agent of the lytic cycle in lysogenic bacteria. All tubes were
151 incubated in darkness in two temperature-controlled incubators maintained respectively at ambient

152 temperature for C1, C2, D1 and D2 and at ambient temperature +3 °C for G1 and G2. Samples for
153 HB and viral abundances were collected every 6 h for a total incubation period of 18 h.

154 The estimation of virus-mediated mortality of HB was performed according to Weinbauer et al.
155 (2002) and Winter et al. (2004). Briefly, increase in virus abundance in the control tubes represents
156 lytic viral production (VPL), and an increase in treatments with mitomycin C represents total viral
157 production (VPT), *i.e.*, lytic plus lysogenic, viral production. The difference between VPT and
158 VPL represents lysogenic production (VPLG). The frequency of lytically infected cells (FLIC)
159 and the frequency of lysogenic cells (FLC) were calculated as:

$$160 \text{ FLIC} = 100 \times \text{VPL} / \text{BS} \times \text{HB}_i \quad (1)$$

$$161 \text{ FLC} = 100 \times \text{VPLG} / \text{BS} \times \text{HB}_i \quad (2)$$

162 where HB_i is the initial HB abundance in the viral production experiment and BS is a theoretical
163 burst size of 20 viruses per infected cell (averaged BS in marine oligotrophic waters, Parada et al.,
164 2006).

165

166 2.4 DNA sampling, sequencing and sequence analysis

167 To study the temporal dynamics of the microbial diversity, water samples (3 L) were
168 collected in acid-washed containers from each minicosm at t_0 , t_{24h} , and at the end of the
169 experiments (t_{72h} at TYR and ION and t_{96h} at FAST). Samples were filtered onto 0.2 μm PES
170 filters (Sterivex©) and stored at -80 °C until DNA extraction. Nucleic acids were extracted from
171 the filters using a phenol-chloroform method and DNA was then purified using filter columns from
172 NucleoSpin® PlantII kit (Macherey-Nagel©) following a modified protocol. DNA extracts were
173 quantified and normalized at 5 ng μL^{-1} and used as templates for PCR amplification of the V4
174 region of the 18S rRNA (~380 bp) using the primers TAREuk454FWD1 and TAREukREV3

175 (Stoeck et al., 2010) and the V4-V5 region of the 16S rRNA (~411 bp) using the primers 515F-Y
176 (5'-GTGYCAGCMGCCGCGGTAA) and 926R-R (5'-CCGYCAATTYMTTTRAGTTT) (Parada
177 et al., 2016). Following polymerase chain reactions, DNA amplicons were purified, quantified and
178 sent to Genotoul (<https://www.genotoul.fr/>, Toulouse, France) for high throughput sequencing
179 using paired-end 2x250bp Illumina MiSeq. Note that although we used universal primer, Archaea
180 were mostly not detected and the prokaryotic heterotrophic communities corresponded essentially
181 to Eubacteria, therefore the taxonomic description referred to the general term 'bacterial
182 communities'

183 All reads were processed using the Quantitative Insight Into Microbial Ecology 2 pipeline
184 (QIIME2 v2020.2, Bolyen et al., 2019). Reads were truncated 350bp based on sequencing
185 quality, denoised, merged and chimera-checked using DADA2 (Callahan et al., 2016). A total of
186 714 and 3070 amplicon sequence variants (ASVs) were obtained for 16S and 18S respectively.
187 Taxonomy assignments were made against the database SILVA 132 (Quast et al., 2013) for 16S
188 and PR2 (Guillou et al., 2013) for 18S. All sequences associated with this study have been
189 deposited under the BioProject ID: PRJNA693966.

190 2.5 Statistics

191 Alpha and beta-diversity indices for community composition were estimated after
192 randomized subsampling to 26000 reads for 16S rDNA and 19000 reads for 18S rDNA. Analysis
193 were run in QIIME 2 and in Primer v.6 software package (Clarke and Warwick, 2001).
194 Differences between the samples richness and diversity were assessed using Kruskal-Wallis
195 pairwise test. Beta diversity was run on Bray Curtis dissimilarity. Differences between samples'
196 beta diversity were tested using PERMANOVA (Permutational Multivariate Analysis of
197 Variance) with pairwise test and 999 permutations. The sequences contributing most to the

198 dissimilarity between clusters were identified using SIMPER (similarity percentage). A linear
199 mixed model was performed using the R software (R Core Team, 2020) using the 'nlme'
200 package (Pinheiro et al., 2014) to test if the amended treatments differed from the controls at
201 t24h and t72h or t96h.

202 3. Results

203 3.1. Microbial growth, mortality and top-down controls

204 Nutrients inputs were observed with dust addition (Fig. S2) and in response the
205 autotrophic and heterotrophic microbial abundances increased, as well as BP (Fig. S3), as
206 described in more details in Gazeau et al (2021a, b). Already 24h following dust addition,
207 significant increases in heterotrophic bacterial biomass specific growth rates (BBGR, $p \leq 0.016$
208 at t24 h) were observed in all experiments with dust under D and G as seen in Fig. 1 (showing
209 data normalized to C) and Fig. S4. The highest growth rates were observed already 24 h after
210 dust seeding (up to 2.9 d^{-1} in G2 at FAST, Table S1, Fig.S4). At 24h, in both D and G,
211 heterotrophic bacterial mortality rates were higher than in C (Fig. 1), especially at TYR in D (up
212 0.5 d^{-1}) and in G at ION (up to 0.6 d^{-1}) and FAST (up to 0.7 d^{-1} , Table S1). Over the course of the
213 three experiments, the slope of the linear regression between log bacterial biomass and log
214 bacterial production was below 0.4 in the three treatments suggesting a weak bottom up control
215 (Fig. 2A; Ducklow, 1992). The slope decreased in D and G relative to C. Overall, the top-down
216 index, as described by Morán et al. (2017), was higher in G (0.92) relative to C and D (0.80).
217 The relationship between log transformed HNF and log bacterial abundance (Fig. 3B), plotted
218 according to the model in Gasol (1994), showed that HNF were below the MRA (Mean realized
219 HNF abundance) in all treatments, suggesting a top-down control of HNF abundance. HNF and
220 bacteria were weakly coupled in all treatments. The relationship between total viruses and
221 bacterial abundance was weaker in D and G relative to C (Fig. S5).

222

223 3.2. Viral dynamics and processes

224 The initial abundance and production of virus-like particles (VLP) was higher in the
225 western stations (Table 1). Viral strategy (lysogenic vs. lytic replication) was also different
226 between stations, with a higher frequency of lysogenic cells (FLC) at TYR and ION (23 and
227 19%, respectively, Table 1) and a higher frequency of lytically infected cells (FLIC) at FAST
228 (43%, Table 1).

229 During TYR and ION experiments, the relative contribution of VLP populations was similar
230 and stable over time with Low DNA viruses representing over 80% of the community (Figs. 3
231 and S5). The Low DNA VLP abundance was however slightly higher in D and G relative to C
232 after 24 h at TYR and significantly higher at ION after 48h ($p = 0.037$; Fig. 4). In contrast to the
233 other two stations, at FAST, Giruses (giant viruses, characterized by high DNA fluorescence and
234 high SSC) were also present and increased in all treatments but especially in G where they made
235 up to 9% of the viral community at the end of the experiment (Figs. 3 and 4). The abundance of
236 high DNA viruses at FAST also increased independent of treatments and accounted for 16 – 18%
237 of the community at the end of the experiment (Figs. 3 and 4).

238 The sampling strategy for production and life strategies of HB viruses allowed to
239 discriminate independently the effect of i) greenhouse conditions (sampling at T0 before dust
240 addition), ii) dust addition (sampling at t24h) and the combined effects of dust addition and
241 greenhouse. Lytic viral production (VPL) increased significantly at T0 in G at TYR and ION
242 compared to C ($p \leq 0.036$). The addition of dust induced higher VPL in D at TYR (normalized to
243 C, Fig.1). No significant impact of dust on VPL was observed in G compared to D after 24h for
244 any of the experiments. Changes in viral infection strategy were observed with G conditions at
245 T0 where FLC decreased relative to the non-G treatments at TYR and ION, and especially at
246 FAST (Fig. 1, $p = 0.047$). FLIC increased slightly in G at TYR and ION already at T0. Dust

247 addition had no detectable significant effect on this parameter for any experiments. Looking at
248 the relative share between lytic and lysogenic infection, dust addition favored lytic infection at
249 TYR (no lysogenic bacteria were observed after 24h) but the contribution of both infection
250 strategies remained unchanged compared to C at ION and FAST. Greenhouse conditions also
251 favored replication through lytic cycle already at T0 for all three experiments and this trend was
252 not impacted by dust addition.

253 3.3. Microbial community composition

254 Microbial community structure, bacteria and micro-eukaryotes from 16S rDNA and 18S
255 rDNA sequencing respectively, responded to dust addition in all three experiments relative to C
256 (Figs. 5 and 6). After quality controls, reads were assigned to 714 and 1443 ASVs for 16S and
257 18S respectively.

258 *3.3.1. Bacterial community composition*

259 The initial community composition (t-12h) was significantly different at the three stations
260 (PERMANOVA; $p = 0.001$, Fig. S6a, S7). Rapid and significant changes in the bacterial
261 community composition were observed already 24 h after dust addition (Fig. 4). Despite the
262 initial different communities, the three stations appeared to converge towards a closer
263 community composition in response to dust addition (Fig. S7). At TYR, communities in D and G
264 significantly changed 24 h after dust addition (PERMANOVA; $p = 0.001$). This cluster presented
265 no significant differences between treatments (D and G) or time (24 and 72 h). The differences
266 between C and D/G were attributed to a relative increase of ASVs related to different
267 *Alteromonas* sp., OM60 and *Pseudophaeobacter* sp. and *Erythrobacter* sp.; contribution of
268 ASVs related to SAR11 and Verrucomicrobia and *Synechococcus* decreased (Table S2a). At

269 ION, the bacterial community composition significantly changed 24 h after dust addition
270 (PERMANOVA; $p = 0.001$) and was significantly different between D and G (PERMANOVA; p
271 $= 0.032$). As observed at TYR, no further change occurred between 24 h and the end of the
272 experiment (72 h; Fig. 5). The difference between the controls and dust amended minicosms
273 were assigned to an increase of ASVs related to different *Alteromonas* sp., *Erythrobacter* sp.,
274 *Dokdonia* sp. and OM60, and a decrease of ASVs related to SAR11, *Synechococcus*,
275 Verrucomicrobia, Rhodospirillales and some Flavobacteria (Table S2b). Several ASVs related to
276 *Alteromonas* sp., *Synechococcus* sp. and *Erythrobacter* sp. were further enriched in G compared
277 D while *Dokdonia* sp. was mainly present in D. At FAST, the bacterial community after 24 h
278 only significantly changed in G (PERMANOVA; $p = 0.011$; Fig. 5). However, after 96 h, the
279 community in D and G were similar and appeared to transition back to the initial state at 96 h
280 (PERMANOVA; $p = 0.077$). The higher relative abundance in *Erythrobacter* sp., *Synechococcus*
281 sp., different ASVs related to *Alteromonas* sp. and Flavobacteria appeared to contribute mainly
282 to the difference between C and D/G (Table S2) while ASVs related to SAR11,
283 Verrucomicrobia, *Celeribacter* sp. *Thalassobius* sp. and Rhodospirillales were mainly present in
284 C (Table S2c).

285 3.3.2 Nano- and micro-eukaryotes community composition

286 The diversity of initial community was large (Fig. S7) and significantly different at the three
287 stations (PERMANOVA; $p = 0.001$; Fig. S6b). At TYR, the nano- and micro-eukaryotes
288 community responded rapidly (24 h) to dust addition (PERMANOVA; $p = 0.003$). This initial
289 high diversity disappeared after 72 h, with similar communities in all minicosms (Fig. S7). They
290 were significantly different from initial and t24h communities ($p = 0.002$ and 0.03 respectively;
291 Fig 6) in D/G. The variations at t24h were attributed to changes in the dinoflagellate

292 communities in particular to an increase in ASVs related to *Heterocapsa rotundata*,
293 Gymnodiniales and Gonyaulacales as well as to an increase in Chlorophyta (Table S3a). At ION,
294 no significant changes were observed between C and D/G after 24 h. However, after 72 h, the
295 communities were significantly different in D ($p = 0.018$) and G ($p = 0.05$) compared to the
296 communities at t24h in these treatments (Table S3b). In D, diversity was significantly higher at
297 t72h compared to t24h and to C at the same sampling time ($p = 0.036$). In contrast, diversity in G
298 at t72h was lower than at t24h and lower to the one observed in C at the same sampling time ($p =$
299 0.066 ; Fig S8). These differences were mainly attributed to changes in ASVs related to
300 dinoflagellates and to the increase at t72h of *Emiliana huxleyi* and Chlorophyta in D and G,
301 respectively (Table S3b). At FAST, significant differences were observed between the controls
302 and initial communities compared to the dust amended (D and G) treatments at t24h ($p = 0.036$).
303 No major differences were observed between D/G at t24h and t96h ($p = 0.06$). The differences
304 were mainly attributed to changes in dinoflagellates ASVs and to an increase in Acantharea and
305 *Emiliana huxleyi* in D and G treatments at t96h (Table S3c).

306 4. Discussion

307 Pulsed inputs of essential nutrients and trace metals through aerosol deposition are crucial to
308 surface microbial communities in LNLC regions such as the Mediterranean Sea (reviewed in
309 Guieu and Ridame, 2020). Here we assessed the impact of dust deposition on the late spring
310 microbial loop under present and future environmental conditions on the surface water of three
311 different Mediterranean basins (Tyrrhenian, TYR; Ionian, ION; and Algerian, FAST). The initial
312 conditions at the three sampled stations for the onboard experiments are described in more
313 details in Gazeau et al. (2021a). Briefly, very low levels of dissolved inorganic nutrients were
314 measured at all three stations, highlighting the oligotrophic status of the waters. This is typical of
315 the stratified conditions generally observed in the Mediterranean Sea in late spring/early summer
316 (*e.g.*, Bosc et al., 2004; D'Ortenzio et al., 2005). Despite similar total chl. *a* concentrations at the
317 three stations (Gazeau et al., 2021a), PP was higher at FAST (Table 1, Gazeau et al., 2021b;
318 Marañón et al., 2021). The initial microbial communities differed substantially between the three
319 stations as shown by pigments (Gazeau et al., 2021a), 18S and 16S rDNA sequencing (this
320 study). DOC concentrations were slightly higher at TYR where PP was the lowest (Gazeau et al.,
321 2021b). HB, HNF abundances (Gazeau et al., 2021a), as well as viral abundance and production
322 increased following the east to west gradient of the initial water conditions.

323 The dust addition induced similar nitrate + nitrite (NO_x) and dissolved inorganic phosphate
324 (DIP) release during all three experiments. Rapid changes were observed on plankton stocks
325 (autotroph and heterotroph abundances and chl.*a*, Gazeau et al., 2021a) and metabolisms (BP
326 and PP, Gazeau et al., 2021b), suggesting that the impact of dust deposition is constrained by the
327 initial composition and metabolic state of the investigated community. While no direct effect of
328 warming and acidification was observed on the amount of nutrient released from dust, Gazeau et

329 al. (2021a, b) showed that biological processes were generally enhanced by these conditions and
330 suggested that deposition may weaken the biological pump in future climate conditions. Here we
331 are further investigating how dust addition in present and future conditions affected, on a short-
332 term scale (≤ 4 days), the microbial trophic interactions and community composition.

333 4.1. Trophic interactions after dust addition under present and future conditions

334 Parallel nutrient enrichment incubations conducted in darkness showed that *in situ*
335 heterotrophic bacterioplankton communities (initial conditions of the present experiments), were
336 N, P co-limited at TYR, mainly P limited at ION and N limited at FAST (Van Wambeke et al.,
337 2021). However, after incubation, the HB appeared to be weakly bottom up controlled
338 (Ducklow, 1992) especially in D and G (Fig 2a) after dust addition. Such top-down control on
339 the bacterioplankton has been previously observed in the Mediterranean Sea, where the
340 bacterioplankton community lives in a dynamic equilibrium between grazing pressure and
341 nutrients limitation, as reviewed by Siokou-Frangou et al., 2010. Moreover, potential increase
342 under future conditions as suggested by the higher top-down index in G ($G = 0.92$ vs. $C/D = 0.80$,
343 Morán et al., 2017) should be further assessed.

344 Bacterial mortality increased relative to controls in D and G at TYR, and only in G at ION
345 and FAST. The weak coupling between bacteria and viruses, as well as the increased virus
346 production and relative abundance of lytic cells (see below), only explained a small fraction of
347 the estimated bacterial mortality (max. 17%), suggesting an additional grazing pressure on
348 bacteria. Nanoflagellates bacterivory can account for up to 87% of bacterial production in the
349 Mediterranean Sea, however rates can be variable in space and time (Siokou-Frangou et al.,
350 2010). Here, HNF abundances increased in D at TYR and at all stations in G (Gazeau et al.,
351 2021a), which could explain the increased bacterial mortality. Increased grazing rate by HNF on

352 bacteria with dust addition has been previously reported in the Eastern Mediterranean Sea
353 (Tsiola et al., 2017). While our results suggest a strong grazing pressure on bacteria, no direct
354 coupling between HNF and bacteria were observed, probably because HNF appeared to be top-
355 down controlled themselves (Gasol, 1994, Fig 3b), potentially by the increasing populations of
356 mixotrophic dinoflagellates and/or Givuses (see below), this suggest intensification of trophic
357 cascades in the microbial loop with nutrient input. It is also possible that HB were grazed by
358 mixotrophic nanoflagellates or by larger protozoans, or that the HNF abundance was
359 underestimated by flow cytometry. Towards the end of the experiment bacterial growth and
360 mortality may also have been linked to DIP depletion at TYR and ION.

361 Considering the seasonal impact of grazing and viral mortality in the Mediterranean Sea,
362 where higher grazing pressure and lysogeny were observed in the stratified nutrient-limited
363 waters in summer (Sánchez et al., 2020), it will be important to further study the seasonal impact
364 of dust deposition on trophic interactions and indirect cascading impact on microbial dynamics
365 and community composition.

366

367 4.2. Viral processes and community during dust enrichment in present and future conditions

368 Viruses represent pivotal components of the marine food web, influencing genome evolution,
369 community dynamics, and ecosystem biogeochemistry (Suttle, 2007). The impacts of marine
370 viruses differ depending on whether they establish lytic or lysogenic infections (Zimmerman et
371 al. 2019, Howard-Varona et al. 2017). Understanding how viral infection processes are
372 influenced by changes in environmental conditions, is thus crucial to better constrain microbial
373 mortality and cascading effects on marine ecosystems. Aerosol deposition was already identified

374 as a factor that stimulates virus production and viral induced mortality of bacteria in the
375 Mediterranean Sea (Pulido-Villena et al., 2014; Tsiola et al., 2017) and direct deposition of
376 airborne viruses and viruses attached to dust particles may also affect microbial food webs
377 (Sharoni et al., 2015; Rahav et al., 2020). However, the impact of future environmental
378 conditions remains more controversial (Larsen et al., 2008; Brussaard et al., 2013; Maat et al.,
379 2014; Vaqué et al., 2019; Malits et al., 2021). The combined effect of aerosol deposition and
380 future conditions of temperature and pH on the viral compartment has, to our knowledge, never
381 been investigated.

382 The rapid changes in viral production and lifestyle observed in all three experiments support the
383 idea that the viral component is sensitive to the environmental variability even on short (hourly)-
384 time scales. The dynamics in viral activities was however impacted differently depending on the
385 treatments and the experiments. Viral production increased in D and G at TYR and only in G at
386 ION and FAST. Regarding the G treatments, increase in viral production was detected before
387 dust addition for all three experiments and remained mostly unchanged for the remaining of the
388 incubation. This suggests that water warming, and acidification were responsible for most
389 changes in viral activities while dusts had no detectable impact in such conditions regardless of
390 the studied station. Based on our results, the most likely explanation for observed changes in
391 viral production is an activation of a lysogenic to lytic switch. The factors that result in prophage
392 induction are still not well constrained, but nutrients pulses and elevated temperatures have been
393 identified as potential stressors (Danovaro et al., 2011 and references therein). Consistent with
394 the observation of N, P co-limited bacterial community at TYR, it is likely that nutrients released
395 from dust upon deposition to surface water activate the productive cycle of temperate viruses at
396 this station. Such mechanism was also speculated during another dust addition study (Pulido-

397 Villena et al., 2014). Under future conditions (G), the low proportion of lysogens was associated
398 to higher frequency of lytically infected cells relative to C and D at TYR and ION. These trends
399 probably reflect an indirect effect of enhanced bacterial growth with increased temperature not
400 only on prophage induction (Danovaro et al., 2011; Vaqué et al., 2019; Mojica and Brussaard,
401 2014) but also on the kinetics of lytic infections. Intriguingly, the enhanced viral production did
402 not translate into marked changes in viral abundance. The abundance of Low DNA virus
403 population, which typically comprises virus of bacteria, actually decreased between t0 and t48h
404 pointing to possible viral decay, potentially related to an adsorption onto dust particles
405 (Weinbauer et al., 2009; Yamada et al., 2020) and the potential export of viral particle to deeper
406 water layers (Van Wambeke et al. 2021). While recurrent patterns emerged from this study, the
407 amplitude of viral responses varied between the experiments. At TYR, where heterotrophic
408 metabolism was higher, the dust addition induced higher viral production relative to controls
409 than at the two other sites, which suggests that viral processes, as other microbial processes, are
410 dependent on the initial metabolic status of the water.

411 Overall, no marked changes were observed for viral communities and abundances after dust
412 addition, both under present and future conditions relative to controls, except at FAST where the
413 abundance of Girus population increased significantly in G from t24h until the end of the
414 experiment. Giruses typically comprise large double stranded DNA viruses that infect
415 nanoeukaryotes including photosynthetic (microalgae) and heterotrophic (HNF, amoeba,
416 choanoflagellate) organisms (Brussaard and Martinez, 2008; Needham et al., 2019; Fischer et al.,
417 2010; Martínez et al., 2014). The presence of Giruses at FAST in this treatment might be
418 explained by the increase in nano-eukaryote abundances at t72h and their decline after 96 h of
419 incubation (Gazeau et al., 2021a). The coccolithophore *Emiliana huxleyi* appears as one of the

420 potential host candidates for these Giruses. The abundance of *E. huxleyi* increased in D and G at
421 this station and this phytoplankter is known to be infected by such giant viruses (Jacquet et al.,
422 2002; Schroeder et al., 2002; Pagarete et al., 2011). It is not clear from our results whether
423 increased Girus abundance is due to the greenhouse effect only (as discussed above for viruses of
424 HB) or the combination of dust addition and greenhouse effects. While temperature warming
425 was shown to accelerate viral production in several virus – phytoplankton systems (Mojica and
426 Brussaard 2014, Demory et al. 2017), a temperature-induced resistance to viral infection was
427 specifically observed in *E. huxleyi* (Kendrick et al., 2014). Previous experiments have also
428 reported a negative impact of acidification on *E. huxleyi* virus dynamics (Larsen et al., 2008). By
429 contrast, nutrient release following dust seeding could indirectly stimulate *E. huxleyi* virus
430 production (Bratbak et al., 1993) or induced switching between non-lethal temperate to lethal
431 lytic stage (Knowles et al., 2020) under future conditions. Targeted analyses are of course
432 required to identify the viral populations selected in G and the outcomes of their infection.
433 Nonetheless, this is the first time, to our knowledge, that dust deposition and enhanced
434 temperature and acidification have been shown to induce the proliferation of Giruses. The impact
435 of dust deposition under future environmental conditions on the viral infections processes could
436 have significant consequences for microbial evolution, food web processes, biogeochemical
437 cycles, and carbon sequestration.

438

439 4.3 Microbial community dynamic after dust addition under present and future conditions

440 While changes in bacterial community composition during various type of dust addition
441 experiments have shown only minor transient responses (*e.g.*, Marañón et al., 2010; Hill et al.,
442 2010; Laghdass et al., 2011; Pulido-Villena et al., 2014; Marín-Beltrán et al., 2019), here

443 microbial community structure showed quick, significant and sustained changes in response to
444 dust addition in all three experiments. Similar to other parameters observed during these
445 experiments (discussed above and in Gazeau et al., 2021a, b), the degree of response in terms of
446 community composition was specific to the tested waters.

447 At TYR, where primary production was low, only transient changes after 24 h of incubation
448 were observed, before the micro-eukaryotes community converged back close to initial
449 conditions. In contrast, the bacterial community significantly and rapidly changed after 24 h and
450 remained different after 72 h. At FAST, where the addition of dust appeared to promote
451 autotrophic processes, the micro-eukaryotes community responded quickly 24 h after dust
452 addition, while minor and delayed changes, probably related to the lower growth rates compared
453 to the other tested waters, were observed in the bacterial community. At ION both eukaryotes
454 and bacterial community responded to dust addition. The delayed response of micro-eukaryotes
455 after 72 h compared to the quick bacterial response at 24 h suggests that HB were better at
456 competing for nutrient inputs at this station and that autotrophic processes may be responding to
457 bacterial nutrient regeneration after a lag phase, further suggesting the tight coupling between
458 heterotrophic bacteria and phytoplankton at this station. The combined effect of decreased pH
459 and elevated temperature on marine microbes is not yet well understood (reviewed in O'Brien et
460 al., 2016). The absence of significant community changes at TYR and FAST while changes were
461 observed at ION, suggests that the response might be dependent on other environmental factors,
462 which need to be further studied.

463 Dust addition likely favors certain group of micro-organisms, suggesting a quicker response
464 of fast growing/copiotrophic groups as well as the increase of specialized functional groups (Guo
465 et al., 2016; Westrich et al., 2016; Maki et al., 2016). Potential toxicity effects of metals and

466 biological particles released from dust/aerosols on certain micro-organisms have also been
467 reported (Paytan et al., 2009; Rahav et al., 2020). Here, the micro-eukaryotic community was
468 dominated by a diverse group of dinoflagellates which were responsible for the main variations
469 between treatments at all stations. The overwhelming abundance of dinoflagellates sequences
470 over other micro-eukaryotes could be biased by the large genomes and multiple ribosomal gene
471 copies per genome found in dinoflagellates (Zhu et al., 2005) or due to their preferential
472 amplification. However, the dominance of dinoflagellates in surface water at this time of the year
473 in the Mediterranean Sea is not uncommon (García-Gómez et al., 2020) and was also observed in
474 surface waters of the three sampled stations by Imaging Flow Cytobot (Marañón et al., 2021).
475 While pigment data suggest an increase of haptophytes and pelagophytes in D (Gazeau et al.,
476 2021a), the sequencing data only show the presence of *Emiliana huxleyi* as responsible for some
477 of the community changes after dust addition at ION and FAST. These pigments could also
478 indicate the presence of dinoflagellates through tertiary endosymbiosis, in particular
479 *Karlodinium* sp. (Yoon et al., 2002; Zapata et al., 2012), which is an important mixotrophic
480 dinoflagellate (Calbet et al., 2011) observed in D and G at ION and FAST. The variations in
481 dinoflagellate groups might have important trophic impacts due to their diverse mixotrophic
482 states (Stoecker et al., 2017) and the effect of dust addition on mixotrophic interactions should be
483 further studied to better understand the cascading impact of dust on food webs and the biological
484 pump.

485 Positive to toxic impacts on cyanobacteria have been reported from atmospheric deposition
486 experiments (e.g., Paytan et al., 2009; Zhou et al., 2021, Rahav et al., 2020). Here,
487 *Synechococcus* appeared to be inhibited at TYR while it was enhanced at ION and FAST,
488 especially under future conditions (this study, Gazeau et al., 2021a). The same ASVs appeared to

489 be inhibited at TYR and ION while promoted at FAST and a different ASVs increased at ION.
490 *Synechococcus* has recently been shown to be stimulated by wet aerosol addition in P-limited
491 conditions but inhibited in N-limited conditions, in the South China Sea (Zhou et al., 2021). It
492 was also shown to be repressed by dust addition in nutrient limited tropical Atlantic (Marañón et
493 al., 2010). This suggests that different *Synechococcus* ecotypes (Sohm et al., 2016) might
494 respond differently to dust addition depending on the initial biogeochemical conditions of the
495 water.

496 In the three experiments, the main bacterial ASVs responsible for the differences between
497 the control and treatments were closely related to different *Alteromonas* strains. *Alteromonas* are
498 ubiquitous in marine environment and can respond rapidly to nutrient pulses (López-Pérez and
499 Rodríguez-Valera, 2014). Some *Alteromonas* are capable to grow on a wide range of carbon
500 compounds (Pedler et al., 2014). They can produce iron binding ligands (Hogle et al., 2016) to
501 rapidly assimilate Fe released from dust. Thus, they could have significant consequences for the
502 marine carbon and Fe cycles during dust deposition events. Other copiotrophic γ -Proteobacteria,
503 such as *Vibrio*, have been observed to bloom after dust deposition in the Atlantic Ocean
504 (Westrich et al., 2016). Guo et al. (2016) using RNA sequencing, also show that γ -Proteobacteria
505 quickly outcompete α -Proteobacteria (mainly SAR11 and Rhodobacterales) that were initially
506 more active. Here, while SAR11 relative abundance decreased in all experiments after 24h, other
507 α -Proteobacteria related to the aerobic anoxygenic phototroph (AAP) *Erythrobacter* sp.,
508 increased in response to dust, in particular under future conditions. Other AAP, such as OM60,
509 also responded to dust addition in our experiment and in the Eastern Mediterranean Sea (Guo et
510 al., 2016). Moreover, bacteriochlorophyll a, a light harvesting pigment present in AAP, was
511 generally higher in dust addition treatments especially under future conditions compared to

512 controls (Fig. S9). Fast growing AAP might quickly outcompete other HB by supplementing
513 their growth with light derived energy (*e.g.*, Koblížek, 2015). They have also been shown to be
514 stimulated by higher temperature (Sato-Takabe et al., 2019). AAP response to dust and future
515 conditions could have a significant role in marine biogeochemical cycles.

516 **5. Conclusion**

517 The microbial food web response to dust addition was dependent on the initial state of the
518 microbial community in the tested waters. A different response in trophic interactions and
519 community composition of the microbial food web, to the wet dust addition, was observed at
520 each station. Generally greater changes were observed in future conditions. Pulsed input of
521 nutrients and trace metals changed the microbial ecosystem from bottom-up limited to a top-
522 down controlled bacterial community, likely from grazing and induced lysogeny. The
523 composition of mixotrophic microeukaryotes and phototrophic prokaryotes was also altered.

524 Overall, the impact of such simulated pulsed nutrient deposition will depend on the initial
525 biogeochemical conditions of the ecosystem, with likely possible large impact on microbial
526 trophic interactions, in particular viral processes, and community structure. All effects might be
527 generally enhanced in future climate scenarios. The impact of dust deposition on metabolic
528 processes and consequences for the carbon and nitrogen cycles and the biological pump based on
529 these minicosm experiments are further discussed in Gazeau et al. (2021b) and Ridame et al.
530 (2021), and the *in situ* effect of a wet dust deposition event is explored in Van Wambeke et al.
531 (2021), in this special issue.

532 **6. Data availability**

533 All data and metadata will be made available at the French INSU/CNRS LEFE CYBER database
534 (scientific coordinator: Herve Claustre; data manager, webmaster: Catherine Schmechtig;
535 INSU/CNRS LEFE CYBER, 2020). All sequences associated with this study have been
536 deposited under the BioProject ID: PRJNA693966.

537

538 **7. Author contributions**

539 FG and CG designed the experiment. All authors participated in sampling or sample
540 processes. JD analyzed the data and wrote the paper with contributions from all authors.

541 **8. Competing interests**

542 The authors declare that they have no conflict of interest.

543 **9. Financial support**

544 This study is a contribution to the PEACETIME project (<http://peacetime-project.org>,
545 <https://doi.org/10.17600/17000300>), a joint initiative of the MERMEX and ChArMEx
546 components supported by CNRS-INSU, IFREMER, CEA, and Météo-France as part of the
547 programme MISTRALS coordinated by INSU. PEACETIME was endorsed as a process study
548 by GEOTRACES and SOLAS. Part of this research was funded by the ANR CALYPSO
549 attributed to ACB (ANR-15-CE01-0009). EM was supported by the Spanish Ministry of Science,
550 Innovation and Universities through grant PGC2018-094553B-I00. JD was funded by a Marie
551 Curie Actions-International Outgoing Fellowship (PIOF-GA-2013-629378).

552

553 **10. Acknowledgements**

554 We gratefully acknowledge the onboard support from the captain and crew of the RV Pourquoi
555 Pas? and of our chief scientists C. Guieu and K. Desboeuf. We also thank K. Djaoudi, J. Uitz, C.
556 Dimier, P. Catala, B. Marie and M. Perez-Lorenzo with their assistance in sampling and analysis
557 of pigments, microbial abundance, DOC concentration and primary production. We thank the
558 two referees for their inputs.

559

560 **11. References**

561 Allen, R., Hoffmann, L. J., Law, C. S., and Summerfield, T. C.: Subtle bacterioplankton
562 community responses to elevated CO₂ and warming in the oligotrophic South Pacific gyre, *Env*
563 *Microbiol Rep*, 12, 377-386, <https://doi.org/10.1111/1758-2229.12844>, 2020.

564 Bolyen, E., Rideout, J. R., Dillon, M. R., Bokulich, N. A., Abnet, C. C., Al-Ghalith, G. A.,
565 Alexander, H., Alm, E. J., Arumugam, M., Asnicar, F., Bai, Y., Bisanz, J. E., Bittinger, K.,
566 Brejnrod, A., Brislawn, C. J., Brown, C. T., Callahan, B. J., Caraballo-Rodríguez, A. M.,
567 Chase, J., Cope, E. K., Da Silva, R., Diener, C., Dorrestein, P. C., Douglas, G. M., Durall, D.
568 M., Duvallet, C., Edwardson, C. F., Ernst, M., Estaki, M., Fouquier, J., Gauglitz, J. M.,
569 Gibbons, S. M., Gibson, D. L., Gonzalez, A., Gorlick, K., Guo, J., Hillmann, B., Holmes, S.,
570 Holste, H., Huttenhower, C., Huttley, G. A., Janssen, S., Jarmusch, A. K., Jiang, L., Kaehler,
571 B. D., Kang, K. B., Keefe, C. R., Keim, P., Kelley, S. T., Knights, D., Koester, I., Kosciolk,
572 T., Kreps, J., Langille, M. G. I., Lee, J., Ley, R., Liu, Y.-X., Loftfield, E., Lozupone, C.,
573 Maher, M., Marotz, C., Martin, B. D., McDonald, D., McIver, L. J., Melnik, A. V., Metcalf, J.
574 L., Morgan, S. C., Morton, J. T., Naimey, A. T., Navas-Molina, J. A., Nothias, L. F.,
575 Orchanian, S. B., Pearson, T., Peoples, S. L., Petras, D., Preuss, M. L., Pruesse, E., Rasmussen,
576 L. B., Rivers, A., Robeson, M. S., Rosenthal, P., Segata, N., Shaffer, M., Shiffer, A., Sinha, R.,

577 Song, S. J., Spear, J. R., Swafford, A. D., Thompson, L. R., Torres, P. J., Trinh, P., Tripathi,
578 A., Turnbaugh, P. J., Ul-Hasan, S., van der Hooft, J. J. J., Vargas, F., Vázquez-Baeza, Y.,
579 Vogtmann, E., von Hippel, M., Walters, W., Wan, Y., Wang, M., Warren, J., Weber, K. C.,
580 Williamson, C. H. D., Willis, A. D., Xu, Z. Z., Zaneveld, J. R., Zhang, Y., Zhu, Q., Knight, R.,
581 and Caporaso, J. G.: Reproducible, interactive, scalable and extensible microbiome data
582 science using QIIME 2, *Nat Biotechnol*, 37, 852-857, 10.1038/s41587-019-0209-9, 2019.

583 Bonnet, S., and Guieu, C.: Atmospheric forcing on the annual iron cycle in the Western
584 Mediterranean Sea: A 1-year survey, *J Geophys Res-Oceans*, 111,
585 <https://doi.org/10.1029/2005JC003213>, 2006.

586 Bosc, E., Bricaud, A., and Antoine, D.: Seasonal and interannual variability in algal biomass and
587 primary production in the Mediterranean Sea, as derived from 4 years of SeaWiFS
588 observations, *Global Biogeochem Cy*, 18, <https://doi.org/10.1029/2003GB002034>, 2004.

589 Bratbak, G., Egge, J. K., and Heldal, M.: Viral mortality of the marine alga *Emiliania huxleyi*
590 (Haptophyceae) and termination of algal blooms, *Mar Ecol Prog Ser*, 39-48, 1993.

591 Brussaard, C., Noordeloos, A., Witte, H., Collenteur, M., Schulz, K. G., Ludwig, A., and
592 Riebesell, U.: Arctic microbial community dynamics influenced by elevated CO₂ levels,
593 *Biogeosciences*, 10, 719-731, 2013.

594 Brussaard, C. P., and Martinez, J. M.: Algal bloom viruses, *Plant Viruses*, 2, 1-13, 2008.

595 Brussaard, C. P. D.: Optimization of Procedures for Counting Viruses by Flow Cytometry, *Appl*
596 *Environ Microb*, 70, 1506-1513, 10.1128/aem.70.3.1506-1513.2004, 2004.

597 Calbet, A., Bertos, M., Fuentes-Grünwald, C., Alacid, E., Figueroa, R., Renom, B., and Garcés,
598 E.: Intraspecific variability in *Karlodinium veneficum*: growth rates, mixotrophy, and lipid
599 composition, *Harmful Algae*, 10, 654-667, 2011.

600 Callahan, B. J., McMurdie, P. J., Rosen, M. J., Han, A. W., Johnson, A. J. A., and Holmes, S. P.:
601 DADA2: High-resolution sample inference from Illumina amplicon data, *Nat Methods*, 13,
602 581, [10.1038/nmeth.3869](https://doi.org/10.1038/nmeth.3869), 2016.

603 Christaki, U., Courties, C., Massana, R., Catala, P., Lebaron, P., Gasol, J. M., and Zubkov, M.
604 V.: Optimized routine flow cytometric enumeration of heterotrophic flagellates using
605 SYBR Green I, *Limnol. Oceanogr-Meth*, 9, 329–339,
606 <https://doi.org/10.4319/lom.2011.9.329>, 2011.

607

608 Clarke, K. R., and Warwick, P. E.: *Change in Marine Communities: An Approach to Statistical*
609 *Analysis and Interpretation*, Plymouth, Ltd ed., 2001.

610 D'Ortenzio, F., Iudicone, D., de Boyer Montegut, C., Testor, P., Antoine, D., Marullo, S.,
611 Santoleri, R., and Madec, G.: Seasonal variability of the mixed layer depth in the
612 Mediterranean Sea as derived from *in situ* profiles, *Geophys Res Let*, 32,
613 <https://doi.org/10.1029/2005GL022463>, 2005.

614 Danovaro, R., Corinaldesi, C., Dell'Anno, A., Fuhrman, J. A., Middelburg, J. J., Noble, R. T.,
615 and Suttle, C. A.: Marine viruses and global climate change, *FEMS Microbiol Rev*, 35, 993-
616 1034, [10.1111/j.1574-6976.2010.00258.x](https://doi.org/10.1111/j.1574-6976.2010.00258.x), 2011.

617 Degerman, R., Dinasquet, J., Riemann, L., Sjøstedt de Luna, S., and Andersson, A.: Effect of
618 resource availability on bacterial community responses to increased temperature, *Aquat Microb*
619 *Ecol*, 68: 131-142, 2012.

620 Desboeufs, K., Leblond, N., Wagener, T., Bon Nguyen, E., and Guieu, C.: Chemical fate and
621 settling of mineral dust in surface seawater after atmospheric deposition observed from dust

622 seeding experiments in large mesocosms, *Biogeosciences*, 11, 5581-5594, 10.5194/bg-11-
623 5581-2014, 2014.

624 Ducklow, H.: Factors regulating bottom-up control of bacteria biomass in open ocean plankton
625 communities, *Arch. Hydrobiol. Beih. Ergebn. Limnol*, 37, 207-217, 1992.

626 Durrieu de Madron, X., Guieu, C., Sempéré, R., Conan, P., Cossa, D., D'Ortenzio, F., Estournel,
627 C., Gazeau, F., Rabouille, C., Stemmann, L., Bonnet, S., Diaz, F., Koubbi, P., Radakovitch, O.,
628 Babin, M., Baklouti, M., Bancon-Montigny, C., Belviso, S., Bensoussan, N., Bonsang, B.,
629 Bouloubassi, I., Brunet, C., Cadiou, J. F., Carlotti, F., Chami, M., Charmasson, S., Charrière,
630 B., Dachs, J., Doxaran, D., Dutay, J. C., Elbaz-Poulichet, F., Eléaume, M., Eyrolles, F.,
631 Fernandez, C., Fowler, S., Francour, P., Gaertner, J. C., Galzin, R., Gasparini, S., Ghiglione, J.
632 F., Gonzalez, J. L., Goyet, C., Guidi, L., Guizien, K., Heimbürger, L. E., Jacquet, S. H. M.,
633 Jeffrey, W. H., Joux, F., Le Hir, P., Leblanc, K., Lefèvre, D., Lejeusne, C., Lemé, R., Loÿe-
634 Pilot, M. D., Mallet, M., Méjanelle, L., Mélin, F., Mellon, C., Méricot, B., Merle, P. L., Migon,
635 C., Miller, W. L., Mortier, L., Mostajir, B., Mousseau, L., Moutin, T., Para, J., Pérez, T.,
636 Petrenko, A., Poggiale, J. C., Prieur, L., Pujo-Pay, M., Pulido, V., Raimbault, P., Rees, A. P.,
637 Ridame, C., Rontani, J. F., Ruiz Pino, D., Sicre, M. A., Taillandier, V., Tamburini, C., Tanaka,
638 T., Taupier-Letage, I., Tedetti, M., Testor, P., Thébault, H., Thouvenin, B., Touratier, F.,
639 Tronczynski, J., Ulses, C., Van Wambeke, F., Vantrepotte, V., Vaz, S., and Verney, R.: Marine
640 ecosystems' responses to climatic and anthropogenic forcings in the Mediterranean, *Prog*
641 *Oceanog*, 91, 97-166, <https://doi.org/10.1016/j.pocean.2011.02.003>, 2011.

642 Fischer, M. G., Allen, M. J., Wilson, W. H., and Suttle, C. A.: Giant virus with a remarkable
643 complement of genes infects marine zooplankton, *P Natl Acad Sci* 107, 19508-19513, 2010.

644 García-Gómez, C., Yebra, L., Cortés, D., Sánchez, A., Alonso, A., Valcárcel-Pérez, N., Gómez-
645 Jakobsen, F., Herrera, I., Johnstone, C., and Mercado, J. M.: Shifts in the protist community
646 associated with an anticyclonic gyre in the Alboran Sea (Mediterranean Sea), *FEMS Microbiol*
647 *Ecol*, 96, 10.1093/femsec/fiaa197, 2020.

648 Gasol, J. M.: A framework for the assessment of top-down vs bottom-up control of heterotrophic
649 nanoflagellate abundance, *Mar ecol prog ser.* 113, 291-300, 1994.

650 Gasol, J.M., and del Giorgio, P.A.: Using flow cytometry for counting natural planktonic
651 bacteria and understanding the structure of the planktonic bacterial communities, *Scientia Mar.*
652 64, 197-224, 2000

653 Gazeau, F., Ridame, C., Van Wambeke, F., Alliouane, S., Stolpe, C., Irisson, J. O., Marro, S.,
654 Grisoni, J. M., De Liège, G., Nunige, S., Djaoudi, K., Pulido-Villena, E., Dinasquet, J.,
655 Obernosterer, I., Catala, P., and Guieu, C.: Impact of dust enrichment on Mediterranean
656 plankton communities under present and future conditions of pH and temperature: an
657 experimental overview, *Biogeosciences*, 2020, 1-81, 10.5194/bg-2020-202, 2021a

658 Gazeau, F., Van Wambeke, F., Marañón, E., Pérez-Lorenzo, M., Alliouane, S., Stolpe, C.,
659 Blasco, T., Leblond, N., Zäncker, B., Engel, A., Marie, B., Dinasquet, J., and Guieu, C.: Impact
660 of dust addition on the metabolism of Mediterranean plankton communities and carbon export
661 under present and future conditions of pH and temperature, *Biogeosciences*,
662 <https://doi.org/10.5194/bg-2021-20>, 2021b.

663 Guieu, C., Dulac, F., Desboeufs, K., Wagener, T., Pulido-Villena, E., Grisoni, J.-M., Louis, F.,
664 Ridame, C., Blain, S., Brunet, C., Bon Nguyen, E., Tran, S., Labiadh, M., and Dominici, J.-M.:
665 Large clean mesocosms and simulated dust deposition: a new methodology to investigate

666 responses of marine oligotrophic ecosystems to atmospheric inputs, *Biogeosciences*, 7, 2765–
667 2784, <https://doi.org/10.5194/bg-7-2765-2010>, 2010.

668 Guieu, C., Aumont, O., Paytan, A., Bopp, L., Law, C. S., Mahowald, N., Achterberg, E. P.,
669 Marañón, E., Salihoglu, B., Crise, A., Wagener, T., Herut, B., Desboeufs, K., Kanakidou, M.,
670 Olgun, N., Peters, F., Pulido-Villena, E., Tovar-Sanchez, A., and Völker, C.: The significance
671 of the episodic nature of atmospheric deposition to Low Nutrient Low Chlorophyll regions,
672 *Global Biogeochem Cy*, 28, 1179-1198, [10.1002/2014GB004852](https://doi.org/10.1002/2014GB004852), 2014.

673 Guieu, C. and Ridame, C.: Impact of atmospheric deposition on marine chemistry and
674 biogeochemistry, in *Atmospheric Chemistry in the Mediterranean Region: Comprehensive
675 Diagnosis and Impacts*, edited by F. Dulac, S. Sauvage, and E. Hamonou, Springer, Cham,
676 Switzerland, 2020.

677 Guillou, L., Bachar, D., Audic, S., Bass, D., Berney, C., Bittner, L., Boutte, C., Burgaud, G., de
678 Vargas, C., Decelle, J., del Campo, J., Dolan, J. R., Dunthorn, M., Edvardsen, B., Holzmann,
679 M., Kooistra, W. H. C. F., Lara, E., Le Bescot, N., Logares, R., Mahé, F., Massana, R.,
680 Montresor, M., Morard, R., Not, F., Pawlowski, J., Probert, I., Sauvadet, A.-L., Siano, R.,
681 Stoeck, T., Vaultot, D., Zimmermann, P., and Christen, R.: The Protist Ribosomal Reference
682 database (PR2): a catalog of unicellular eukaryote Small Sub-Unit rRNA sequences with
683 curated taxonomy, *Nucleic Acids Res*, 41, D597-D604, [10.1093/nar/gks1160](https://doi.org/10.1093/nar/gks1160), 2013.

684 Guo, C., Xia, X., Pitta, P., Herut, B., Rahav, E., Berman-Frank, I., Giannakourou, A., Tsiola, A.,
685 Tsagaraki, T. M., and Liu, H.: Shifts in Microbial Community Structure and Activity in the
686 Ultra-Oligotrophic Eastern Mediterranean Sea Driven by the Deposition of Saharan Dust and
687 European Aerosols, *Front Mar Sci*, 3, [10.3389/fmars.2016.00170](https://doi.org/10.3389/fmars.2016.00170), 2016.

688 Highfield, A., Joint, I., Gilbert, J. A., Crawford, K. J., and Schroeder, D. C.: Change in *Emiliana*
689 *huxleyi* Virus Assemblage Diversity but Not in Host Genetic Composition during an Ocean
690 Acidification Mesocosm Experiment, *Viruses*, 9, 41, 2017.

691 Hill, P. G., Zubkov, M. V., and Purdie, D. A.: Differential responses of *Prochlorococcus* and
692 SAR11-dominated bacterioplankton groups to atmospheric dust inputs in the tropical Northeast
693 Atlantic Ocean, *FEMS Microbiol Let*, 306, 82-89, 10.1111/j.1574-6968.2010.01940.x, 2010.

694 Hogle, S. L., Bundy, R. M., Blanton, J. M., Allen, E. E., and Barbeau, K. A.: Copiotrophic
695 marine bacteria are associated with strong iron-binding ligand production during
696 phytoplankton blooms, *Limnol Oceanogr Let*, 10.1002/lol2.10026, 2016.

697 Howard-Varona, C., Hargreaves, K., Abedon, S., and Sullivan, M.B.: Lysogeny in nature:
698 mechanisms, impact and ecology of temperate phages, *ISME J*, 11, 1511–1520,
699 10.1038/ismej.2017.16, 2017.

700 Hu, C., Li, X., He, M., Jiang, P., Long, A., and Xu, J.: Effect of Ocean Acidification on Bacterial
701 Metabolic Activity and Community Composition in Oligotrophic Oceans, Inferred From Short-
702 Term Bioassays, *Front Microbiol*, 12, 10.3389/fmicb.2021.583982, 2021.

703 IPCC: Climate Change 2013: The Physical Science Basis. Contribution of Working Group I to
704 the Fifth Assessment Report of the Intergovernmental Panel on Climate Change, Cambridge
705 University Press, Cambridge, United Kingdom and New York, NY, USA, 1535 pp., 2014.

706 Jacquet, S., Heldal, M., Iglesias-Rodriguez, D., Larsen, A., Wilson, W., and Bratbak, G.: Flow
707 cytometric analysis of an *Emiliana huxleyi* bloom terminated by viral infection, *Aquat Microb*
708 *Ecol*, 27, 111-124, 2002.

709 Kendrick, B. J., DiTullio, G. R., Cyronak, T. J., Fulton, J. M., Van Mooy, B. A., and Bidle, K.
710 D.: Temperature-induced viral resistance in *Emiliania huxleyi* (Prymnesiophyceae), PLoS One,
711 9, e112134, 2014.

712 Kirchman, D., Knees, E., and Hodson, R.: Leucine Incorporation and Its Potential As A Measure
713 of Protein-Synthesis by Bacteria in Natural Aquatic Systems, Appl Environ Microbiol, 49,
714 599-607, 1985.

715 Kirchman, D.: Calculating microbial growth rates from data on production and standing stocks,
716 Mar Ecol Prog Ser, 233, 303-306, 2002.

717 Knowles, B., Bonachela, J. A., Behrenfeld, M. J., Bondoc, K. G., Cael, B., Carlson, C. A.,
718 Cieslik, N., Diaz, B., Fuchs, H. L., and Graff, J. R.: Temperate infection in a virus–host system
719 previously known for virulent dynamics, Nat comms, 11, 1-13, 2020.

720 Koblížek, M.: Ecology of aerobic anoxygenic phototrophs in aquatic environments, FEMS
721 Microbiol Rev, 39, 854-870, 10.1093/femsre/fuv032, 2015.

722 Krause, E., Wichels, A., Giménez, L., Lunau, M., Schilhabel, M. B., and Gerdtts, G.: Small
723 Changes in pH Have Direct Effects on Marine Bacterial Community Composition: A
724 Microcosm Approach, PLOS ONE, 7, e47035, 10.1371/journal.pone.0047035, 2012.

725 Laghdass, M., Blain, S., Besseling, M., Catala, P., Guieu, C., and Obernosterer, I.: Effects of
726 Saharan dust on the microbial community during a large *in situ* mesocosm experiment in the
727 NW Mediterranean Sea, Aquat Microb Ecol, 62, 201-213, 2011.

728 Larsen, J. B., Larsen, A., Thyrraug, R., Bratbak, G., and Sandaa, R.-A.: Response of marine
729 viral populations to a nutrient induced phytoplankton bloom at different $p\text{CO}_2$ levels,
730 Biogeosciences, 5, 523-533, 2008.

731 Lee, S. H., and Fuhrman, J. A.: Relationships between biovolume and biomass of naturally
732 derived marine bacterioplankton, *Appl Environ Microbiol*, 53, 1298-1303, 1987.

733 Loÿe-Pilot, M., and Martin, J.: Saharan dust input to the western Mediterranean: an eleven years
734 record in Corsica, in: *The impact of desert dust across the Mediterranean*, Springer, 191-199,
735 1996.

736 López-Pérez, M., and Rodriguez-Valera, F.: The Family Alteromonadaceae, in: *The Prokaryotes:*
737 *Gammaproteobacteria*, edited by: Rosenberg, E., DeLong, E. F., Lory, S., Stackebrandt, E., and
738 Thompson, F., Springer Berlin Heidelberg, Berlin, Heidelberg, 69-92, 2014.

739 Maat, D. S., Crawford, K. J., Timmermans, K. R., and Brussaard, C. P.: Elevated carbon dioxide
740 and phosphorus limitation favor *Micromonas pusilla* through stimulated growth and reduced
741 viral impact, aspects of algal host-virus interactions in a changing ocean, 80, 29, 2014.

742 Mahowald, N. M., Scanza, R., Brahney, J., Goodale, C. L., Hess, P. G., Moore, J. K., and Neff,
743 J.: Aerosol Deposition Impacts on Land and Ocean Carbon Cycles, *Current Climate Change*
744 *Reports*, 3, 16-31, 10.1007/s40641-017-0056-z, 2017.

745 Maki, T., Ishikawa, A., Mastunaga, T., Pointing, S. B., Saito, Y., Kasai, T., Watanabe, K., Aoki,
746 K., Horiuchi, A., Lee, K. C., Hasegawa, H., and Iwasaka, Y.: Atmospheric aerosol deposition
747 influences marine microbial communities in oligotrophic surface waters of the western Pacific
748 Ocean, *Deep Sea Research Part I: Oceanographic Research Papers*, 118, 37-45,
749 <https://doi.org/10.1016/j.dsr.2016.10.002>, 2016.

750 Malits, A., Boras, J.A., Balagué, V., Calvo, E., Gasol, J.M., Marrasé, C., Pelejero, C., Pinhassi,
751 J., Sala, M.M. and Vaqué, D. Viral-Mediated Microbe Mortality Modulated by Ocean
752 Acidification and Eutrophication: Consequences for the Carbon Fluxes Through the Microbial
753 Food Web. *Front. Microbiol.* 12:635821. doi: 10.3389/fmicb.2021.635821, 2021

754 Marañón, E., Fernández, A., Mouriño-Carballido, B., Martínez-García, S., Teira, E., Cermeño,
755 P., Chouciño, P., Huete-Ortega, M., Fernández, E., Calvo-Díaz, A., Morán, X. A. G., Bode, A.,
756 Moreno-Ostos, E., Varela, M. M., Patey, M. D., and Achterberg, E. P.: Degree of oligotrophy
757 controls the response of microbial plankton to Saharan dust, *Limnology and Oceanography*, 55,
758 2339-2352, <https://doi.org/10.4319/lo.2010.55.6.2339>, 2010.

759 Marañón, E., Lorenzo, M. P., Cermeño, P., and Mouriño-Carballido, B.: Nutrient limitation
760 suppresses the temperature dependence of phytoplankton metabolic rates, *The ISME Journal*,
761 12, 1836-1845, 10.1038/s41396-018-0105-1, 2018.

762 Marañón, E., Van Wambeke, F., Uitz, J., Boss, E. S., Pérez-Lorenzo, M., Dinasquet, J.,
763 Haëntjens, N., Dimier, C., and Taillandier, V.: Deep maxima of phytoplankton biomass,
764 primary production and bacterial production in the Mediterranean Sea during late spring,
765 *Biogeosciences Discuss.*, 2020, 1-28, 10.5194/bg-2020-261, 2020.

766 Marín-Beltrán, I., Logue, J. B., Andersson, A. F., and Peters, F.: Atmospheric Deposition Impact
767 on Bacterial Community Composition in the NW Mediterranean, *Frontiers in Microbiology*,
768 10, 10.3389/fmicb.2019.00858, 2019.

769 Martínez, J. M., Swan, B. K., and Wilson, W. H.: Marine viruses, a genetic reservoir revealed by
770 targeted viromics, *The ISME Journal*, 8, 1079-1088, 10.1038/ismej.2013.214, 2014.

771 Mojica, K. D., and Brussaard, C. P.: Factors affecting virus dynamics and microbial host–virus
772 interactions in marine environments, *FEMS microbiology ecology*, 89, 495-515, 2014.

773 Morán, X. A. G., Gasol, J. M., Pernice, M. C., Mangot, J.-F., Massana, R., Lara, E., Vaqué, D.,
774 and Duarte, C. M.: Temperature regulation of marine heterotrophic prokaryotes increases
775 latitudinally as a breach between bottom-up and top-down controls, *Global Change Biology*,
776 23, 3956-3964, <https://doi.org/10.1111/gcb.13730>, 2017.

777 Morán, X. A. G., Baltar, F., Carreira, C., and Lønborg, C.: Responses of physiological groups of
778 tropical heterotrophic bacteria to temperature and dissolved organic matter additions: food
779 matters more than warming, *Environmental Microbiology*, 22, 1930-1943,
780 <https://doi.org/10.1111/1462-2920.15007>, 2020.

781 Moulin, C., and Chiapello, I.: Impact of human-induced desertification on the intensification of
782 Sahel dust emission and export over the last decades, *Geophysical Research Letters*, 33,
783 <https://doi.org/10.1029/2006GL025923>, 2006.

784 Needham, D. M., Yoshizawa, S., Hosaka, T., Poirier, C., Choi, C. J., Hehenberger, E., Irwin, N.
785 A., Wilken, S., Yung, C.-M., and Bachy, C.: A distinct lineage of giant viruses brings a
786 rhodopsin photosystem to unicellular marine predators, *Proceedings of the National Academy*
787 *of Sciences*, 116, 20574-20583, 2019.

788 O'Brien, P. A., Morrow, K. M., Willis, B. L., and Bourne, D. G.: Implications of Ocean
789 Acidification for Marine Microorganisms from the Free-Living to the Host-Associated,
790 *Frontiers in Marine Science*, 3, 10.3389/fmars.2016.00047, 2016.

791 Pagarete, A., Le Corguillé, G., Tiwari, B., Ogata, H., de Vargas, C., Wilson, W. H., and Allen,
792 M. J.: Unveiling the transcriptional features associated with coccolithovirus infection of natural
793 *Emiliana huxleyi* blooms, *FEMS Microbiology Ecology*, 78, 555-564, 10.1111/j.1574-
794 6941.2011.01191.x, 2011.

795 Parada, A. E., Needham, D. M., and Fuhrman, J. A.: Every base matters: assessing small subunit
796 rRNA primers for marine microbiomes with mock communities, time series and global field
797 samples, *Environmental Microbiology*, 18, 1403-1414, 10.1111/1462-2920.13023, 2016.

798 Parada, V., Herndl, G. J., and Weinbauer, M. G.: Viral burst size of heterotrophic prokaryotes in
799 aquatic systems, *JMBA-Journal of the Marine Biological Association of the United Kingdom*,
800 86, 613, 2006.

801 Paytan, A., Mackey, K. R. M., Chen, Y., Lima, I. D., Doney, S. C., Mahowald, N., Labiosa, R.,
802 and Post, A. F.: Toxicity of atmospheric aerosols on marine phytoplankton, *Proceedings of the*
803 *National Academy of Sciences*, 106, 4601-4605, 10.1073/pnas.0811486106, 2009.

804 Pedler, B. E., Aluwihare, L. I., and Azam, F.: Single bacterial strain capable of significant
805 contribution to carbon cycling in the surface ocean, *Proceedings of the National Academy of*
806 *Sciences of the United States of America*, 111, 7202-7207, 2014.

807 Pinheiro, J., Bates, D., DebRoy, S., and Sarkar, D.: R Core Team. nlme: linear and nonlinear
808 mixed effects models. R package version 3.1-117, Available at [http://CRAN.R-project.](http://CRAN.R-project.org/package=nlme)
809 [org/package=nlme](http://CRAN.R-project.org/package=nlme), 2014.

810 Pitta, P., Kanakidou, M., Mihalopoulos, N., Christodoulaki, S., Dimitriou, P.D., Frangoulis, C.,
811 Giannakourou, A., Kagiorgi, M., Lagaria, A., Nikolaou, P., Papageorgiou, N., Psarra, S., Santi,
812 I., Tsapakis, M., Tsiola, A., Violaki, K., and Petihakis, G. Saharan Dust Deposition Effects on
813 the Microbial Food Web in the Eastern Mediterranean: A Study Based on a Mesocosm
814 Experiment. *Front. Mar. Sci.* 4:117. doi: 10.3389/fmars.2017.00117, 2017

815 Pulido-Villena, E., Baudoux, A. C., Obernosterer, I., Landa, M., Caparros, J., Catala, P.,
816 Georges, C., Harmand, J., and Guieu, C.: Microbial food web dynamics in response to a
817 Saharan dust event: results from a mesocosm study in the oligotrophic Mediterranean Sea,
818 *Biogeosciences*, 11, 5607-5619, 10.5194/bg-11-5607-2014, 2014.

819 Quast, C., Pruesse, E., Yilmaz, P., Gerken, J., Schweer, T., Yarza, P., Peplies, J., and Glöckner,
820 F. O.: The SILVA ribosomal RNA gene database project: improved data processing and web-
821 based tools, *Nucleic Acids Research*, 41, D590-D596, 10.1093/nar/gks1219, 2013.

822 R Core Team: R: A language and environment for statistical computing. , R Foundation for
823 Statistical Computing, Vienna, Austria., <https://www.R-project.org/>. 2020.

824 Rahav, E., Paytan, A., Mescioglou, E., Bar-Zeev, E., Martínez Ruiz, F., Xian, P., and Herut, B.:
825 Bio-Aerosols Negatively Affect *Prochlorococcus* in Oligotrophic Aerosol-Rich Marine
826 Regions, *Atmosphere*, 11, 540, 2020.

827 Ridame, C., Le Moal, M., Guieu, C., Ternon, E., Biegala, I. C., L'Helguen, S., and Pujo-Pay, M.:
828 Nutrient control of N₂ fixation in the oligotrophic Mediterranean Sea and the impact of
829 Saharan dust events, *Biogeosciences*, 8, 2773-2783, 10.5194/bg-8-2773-2011, 2011.

830 Ridame, C., Dinasquet, J., Hallstrøm, S., Bigeard, E., Riemann, L., Van Wambeke, F., Bressac,
831 M., Pulido-Villena, E., Taillandier, V., Gazeau, F., Tover-Sanchez, A., Baudoux, A-C., and
832 Guieu, C.: N₂ fixation in the Mediterranean Sea related to the composition of the diazotrophic
833 community, and impact of dust under present and future environmental conditions,
834 *Biogeosciences Discuss.*, <https://doi.org/10.5194/bg-2021-190>, 2021

835 Sánchez, O., Ferrera, I., Mabrito, I., Gazulla, C. R., Sebastián, M., Auladell, A., Marín-Vindas,
836 C., Cardelús, C., Sanz-Sáez, I., Pernice, M. C., Marrasé, C., Sala, M. M., and Gasol, J. M.:
837 Seasonal impact of grazing, viral mortality, resource availability and light on the group-
838 specific growth rates of coastal Mediterranean bacterioplankton, *Scientific Reports*, 10, 19773,
839 10.1038/s41598-020-76590-5, 2020.

840 Sato-Takabe, Y., Hamasaki, K., and Suzuki, S.: High temperature accelerates growth of aerobic
841 anoxygenic phototrophic bacteria in seawater, *MicrobiologyOpen*, 8, e00710-e00710,
842 10.1002/mbo3.710, 2019.

843 Schroeder, D., Oke, J., Malin, G., and Wilson, W.: Coccolithovirus (Phycodnaviridae):
844 characterisation of a new large dsDNA algal virus that infects *Emiliana huxleyi*, *Archives of*
845 *virology*, 147, 1685-1698, 2002.

846 Sharoni, S., Trainic, M., Schatz, D., Lehahn, Y., Flores, M.J., Bidle, K.D., Ben-Dor, S., Rudich,
847 Y., Koren, I. and Vardi, A.: Infection of phytoplankton by aerosolized marine viruses.
848 *Proceedings of the National Academy of Sciences*, 112, 6643-6647, [10.1073/pnas.1423667112](https://doi.org/10.1073/pnas.1423667112),
849 2015.

850 Siokou-Frangou, I., Christaki, U., Mazzocchi, M. G., Montresor, M., Ribera d'Alcalá, M., Vaqué,
851 D., and Zingone, A.: Plankton in the open Mediterranean Sea: a review, *Biogeosciences*, 7,
852 1543-1586, 10.5194/bg-7-1543-2010, 2010.

853 Smith, D. C., and Azam, F.: A simple, economical method for measuring bacterial protein
854 synthesis rates in seawater using ³H-leucine, *Marine microbial food webs*, 6, 102-114, 1992.

855 Sohm, J. A., Ahlgren, N. A., Thomson, Z. J., Williams, C., Moffett, J. W., Saito, M. A., Webb,
856 E. A., and Rocap, G.: Co-occurring *Synechococcus* ecotypes occupy four major oceanic
857 regimes defined by temperature, macronutrients and iron, *The ISME journal*, 10, 333-345,
858 10.1038/ismej.2015.115, 2016.

859 Stoeck, T., Bass, D., Nebel, M., Christen, R., Jones, M. D. M., Breiner, H. W., and Richards, T.
860 A.: Multiple marker parallel tag environmental DNA sequencing reveals a highly complex
861 eukaryotic community in marine anoxic water, *Molecular Ecology*, 19, 21-31, 2010.

862 Stoecker, D. K., Hansen, P. J., Caron, D. A., and Mitra, A.: Mixotrophy in the Marine Plankton,
863 Annual Review of Marine Science, 9, 311-335, 10.1146/annurev-marine-010816-060617,
864 2017.

865 Suttle, C. A.: Marine viruses — major players in the global ecosystem, Nature Reviews
866 Microbiology, 5, 801-812, 10.1038/nrmicro1750, 2007.

867 Ternon, E., Guieu, C., Loÿe-Pilot, M. D., Leblond, N., Bosc, E., Gasser, B., Miquel, J. C., and
868 Martín, J.: The impact of Saharan dust on the particulate export in the water column of the
869 North Western Mediterranean Sea, Biogeosciences, 7, 809-826, 10.5194/bg-7-809-2010, 2010.

870 Tsiola, A., Tsagaraki, T. M., Giannakourou, A., Nikolioudakis, N., Yücel, N., Herut, B., and
871 Pitta, P.: Bacterial Growth and Mortality after Deposition of Saharan Dust and Mixed Aerosols
872 in the Eastern Mediterranean Sea: A Mesocosm Experiment, Frontiers in Marine Science, 3,
873 10.3389/fmars.2016.00281, 2017.

874 Van Wambeke, F., Taillandier, V., Deboeufs, K., Pulido-Villena, E., Dinasquet, J., Engel, A.,
875 Marañón, E., Ridame, C., and Guieu, C.: Influence of atmospheric deposition on
876 biogeochemical cycles in an oligotrophic ocean system, Biogeosciences, 2021

877 Vaqué, D., Lara, E., Arrieta, J. M., Holding, J., Sarà, E. L., Hendriks, I. E., Coello-Camba, A.,
878 Alvarez, M., Agustí, S., Wassmann, P. F., and Duarte, C. M.: Warming and CO₂ Enhance
879 Arctic Heterotrophic Microbial Activity, Frontiers in Microbiology, 10,
880 10.3389/fmicb.2019.00494, 2019.

881 Weinbauer, M., Bettarel, Y., Cattaneo, R., Luef, B., Maier, C., Motegi, C., Peduzzi, P., and Mari,
882 X.: Viral ecology of organic and inorganic particles in aquatic systems: avenues for further
883 research, Aquatic Microbial Ecology, 57, 321-341, 2009.

884 Weinbauer, M. G., Winter, C., and Höfle, M. G.: Reconsidering transmission electron
885 microscopy based estimates of viral infection of bacterio-plankton using conversion factors
886 derived from natural communities, *Aquatic Microbial Ecology*, 27, 103-110, 2002.

887 Weinbauer, M. G., Rowe, J. M., and Wilhelm, S.: Determining rates of virus production in
888 aquatic systems by the virus reduction approach, 2010.

889 Westrich, J. R., Ebling, A. M., Landing, W. M., Joyner, J. L., Kemp, K. M., Griffin, D. W., and
890 Lipp, E. K.: Saharan dust nutrients promote *Vibrio* bloom formation in marine surface waters,
891 *Proceedings of the National Academy of Sciences*, 113, 5964-5969, 10.1073/pnas.1518080113,
892 2016.

893 Winter, C., Herndl, G. J., and Weinbauer, M. G.: Diel cycles in viral infection of
894 bacterioplankton in the North Sea, *Aquatic Microbial Ecology*, 35, 207-216, 2004.

895 Yamada, Y., Guillemette, R., Baudoux, A.-C., Patel, N., and Azam, F.: Viral Attachment to
896 Biotic and Abiotic Surfaces in Seawater, *Applied and Environmental Microbiology*, 86,
897 e01687-01619, 10.1128/aem.01687-19, 2020.

898 Yoon, H. S., Hackett, J. D., and Bhattacharya, D.: A single origin of the peridinin- and
899 fucoxanthin-containing plastids in dinoflagellates through tertiary endosymbiosis, *Proceedings*
900 *of the National Academy of Sciences*, 99, 11724-11729, 10.1073/pnas.172234799, 2002.

901 Zapata, M., Fraga, S., Rodríguez, F., and Garrido, J. L.: Pigment-based chloroplast types in
902 dinoflagellates, *Marine Ecology Progress Series*, 465, 33-52, 2012.

903 Zhou, W., Li, Q. P., and Wu, Z.: Coastal phytoplankton responses to atmospheric deposition
904 during summer, *Limnol Oceanogr*, 66: 1298-1315, 2021.

905 Zhu, F., Massana, R., Not, F., Marie, D., and Vaulot, D.: Mapping of picoeucaryotes in marine
906 ecosystems with quantitative PCR of the 18S rRNA gene, *FEMS microbiology ecology*, 52,
907 79-92, 2005.

908 Zimmerman, A.E., Howard-Varona, C., Needham, D.M., John, S.G., Worden, A.Z., Sullivan,
909 M.B., Waldbauer, J.R., and Coleman, M.L.: Metabolic and biogeochemical consequences of
910 viral infection in aquatic ecosystems, *Nat Rev Microbiol*, 18, 21-34, 10.1038/s41579-019-
911 0270-x, 2020.

912

913

914 **Tables and Figures**

915 **Table1:** Initial conditions (t-12h) at the three stations sampled for the dust addition experiments. Other
 916 parameters are presented in more details in Gazeau et al. (2020; 2021)

Variables	TYR	ION	FAST
Location	Tyrrhenian Basin	Ionian Basin	Algerian Basin
Coordinates	39.34N, 12.60E	35.49N, 19.78E	37.95N, 2.90E
Temperatures (°C)	20.6	21.2	21.5
DOC (µM) ²	72.2	70.2	69.6
Chlorophyll <i>a</i> (µg L ⁻¹) ¹	0.063	0.066	0.072
BP (ng C L ⁻¹ h ⁻¹) ²	11.6	15.1	34.6
Bacterial abundance (x10 ⁵ cells mL ⁻¹) ¹	4.79	2.14	6.15
BBGR (d ⁻¹)	0.03	0.08	0.07
Viral abundance (x 10 ⁶ VLP mL ⁻¹)	3.01	1.44	2.79
% Lysogenic bacteria FLC	22.7	19.4	7.8
% Lytic bacteria FLIC	17.5	37.2	42.7
Viral production (x 10 ⁴ VLP mL ⁻¹ h ⁻¹)	2.05	1.36	7.99
HNF abundance (cells mL ⁻¹) ¹	110	53	126
Diatoms (cells L ⁻¹) ¹	340	900	1460
Dinoflagellates (cells L ⁻¹) ¹	2770	3000	3410
Ciliates (cells L ⁻¹) ¹	270	380	770

917

918 DOC: dissolved organic carbon, BP: heterotrophic prokaryotic production, BBGR: bacterial biomass
 919 specific growth rates, HNF: Heterotrophic nanoflagellates

920 ¹Results presented in Gazeau et al. 2021a

921 ²Results presented in Gazeau et al. 2021b

922

923

924

925

926

927

928

929

930

931

932 **Figure legends:**

933 **Figure 1.** Bacterial and viral parameters in the three experiments (TYR, ION and FAST) in each minicosm
934 (D1, D2, G1 and G2). The values are normalized to the controls: the data are presented as the difference
935 between the treatments and the mean value of the duplicate controls. The first row represents the
936 bacterial biomass specific growth rates (BBGR) and relative mortality rates at t24h after dust addition.
937 The second row represents the relative viral productions at t24h and at T0 for the G treatments. The last
938 row represents the viral strategies: the percentages of lytic (FLIC) or lysogenic (FLC) cells at t24h and at
939 T0 for the G treatments.

940 **Figure 2.** (A) Log-log linear regression between bacterial biomass and bacterial production, dotted lines
941 represent linear regressions for each treatment. (B) Relationships between log HNF abundance and log
942 bacterial prey abundance. Solid black and dotted black lines corresponds to the Mean Realized HNF
943 Abundance (MRA) and theoretical Maximum Attainable HNF Abundance line (MAA) respectively. The
944 samples are grouped per treatments.

945 **Figure 3.** Relative abundance of viral populations at the initial (*in situ*: at t-12h before dust addition) and
946 final time points in all minicosms (C1, C2, D1, D2, G1 and G2) during the three experiments (TYR, ION
947 and FAST).

948 **Figure 4.** Evolution of Virus like particles abundances (VLP) of three different viral populations over the
949 course of the three experiments (TYR, ION and FAST). The first row represents low DNA viruses or
950 phages, the second row represents high DNA viruses, and the third row represents giant viruses
951 (Giruses).

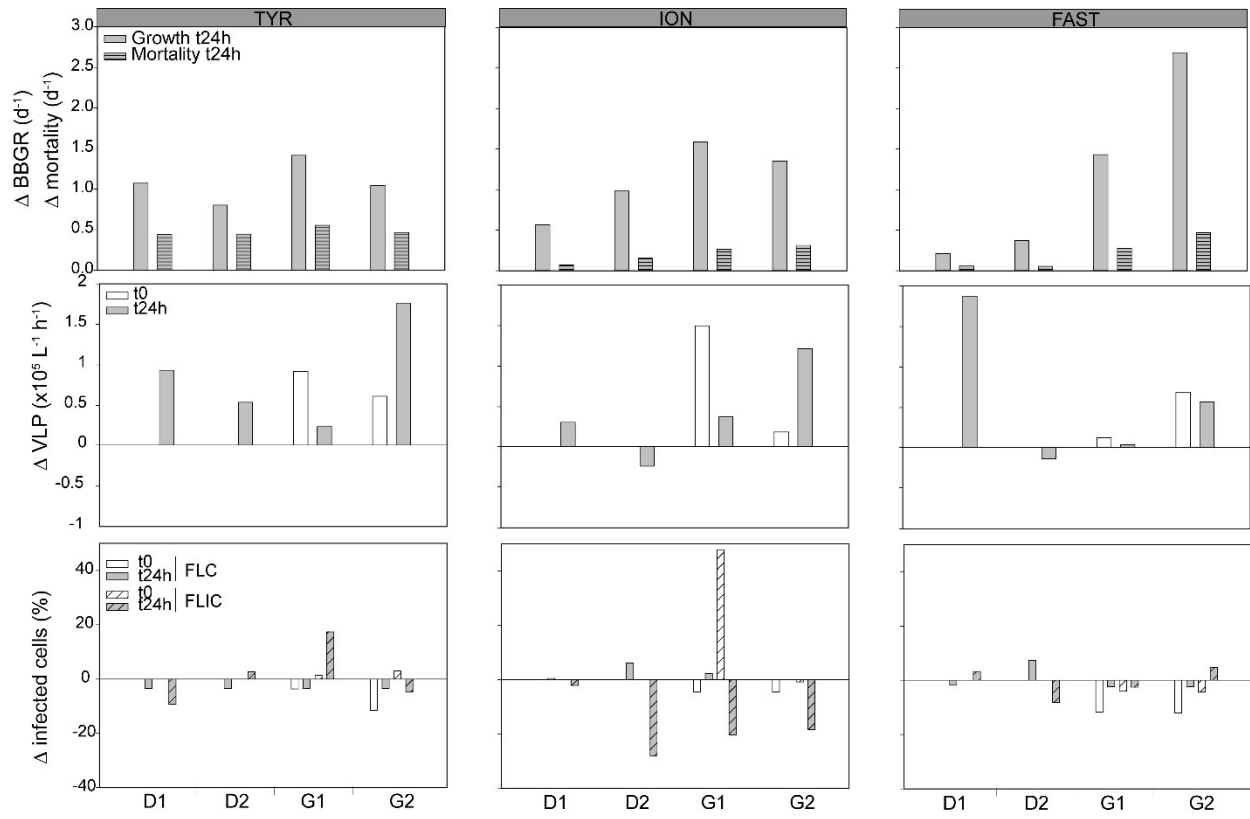
952 **Figure 5.** nMDS plot of bacterial community composition over the course of the three experiments
953 based on Bray-Curtis dissimilarities of 16S rDNA sequences. Samples clustering at different level of
954 similarity are circled together. All circles represent clusters which are significantly different from each
955 other ($p < 0.05$) based on a PERMANOVA test.

956 **Figure 6.** nMDS plot of micro-eukaryotes community composition over the course of the three
957 experiments based on Bray-Curtis dissimilarities of 18S rDNA sequences. Samples clustering at different
958 level of similarity are circled together. All circles represent clusters which are significantly different ($p <$
959 0.05) from each other based on a PERMANOVA test.

960

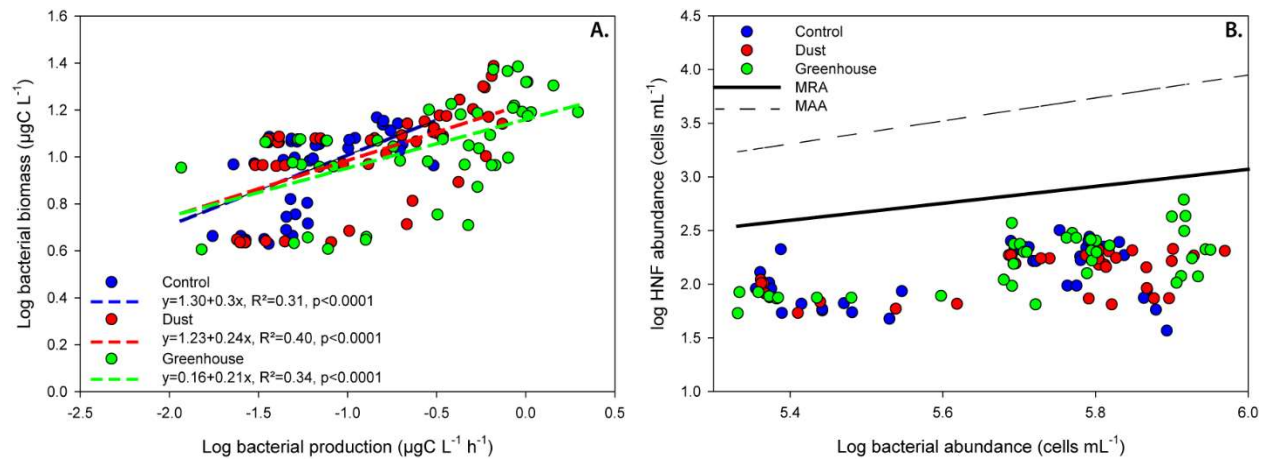
961

962



963

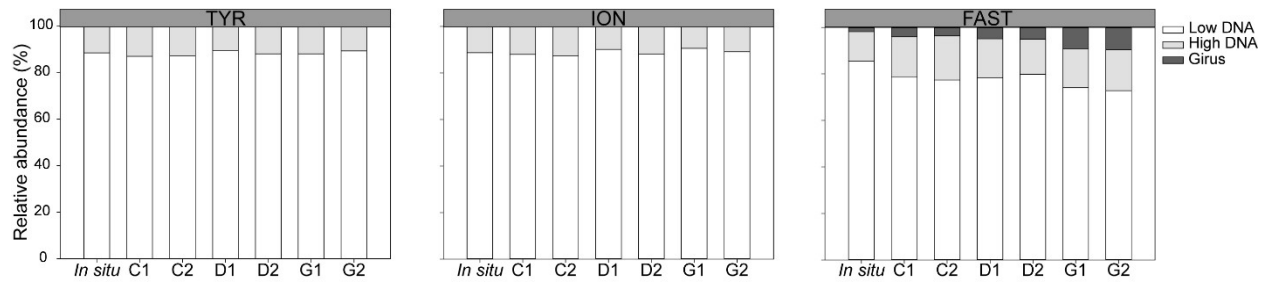
964 **Figure 1.**



965 **Figure 2.**

966

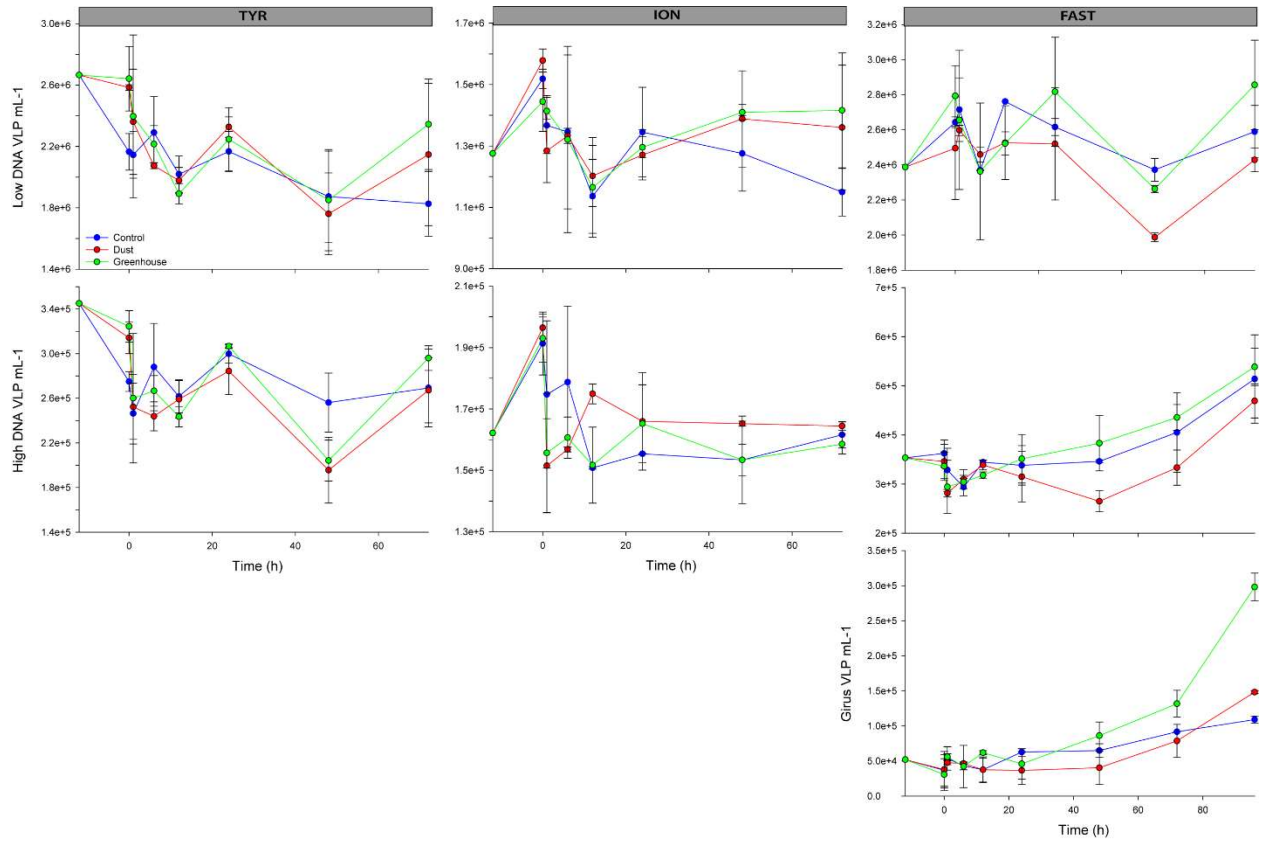
967



968

969 **Figure 3.**

970



971

972 **Figure 4.**

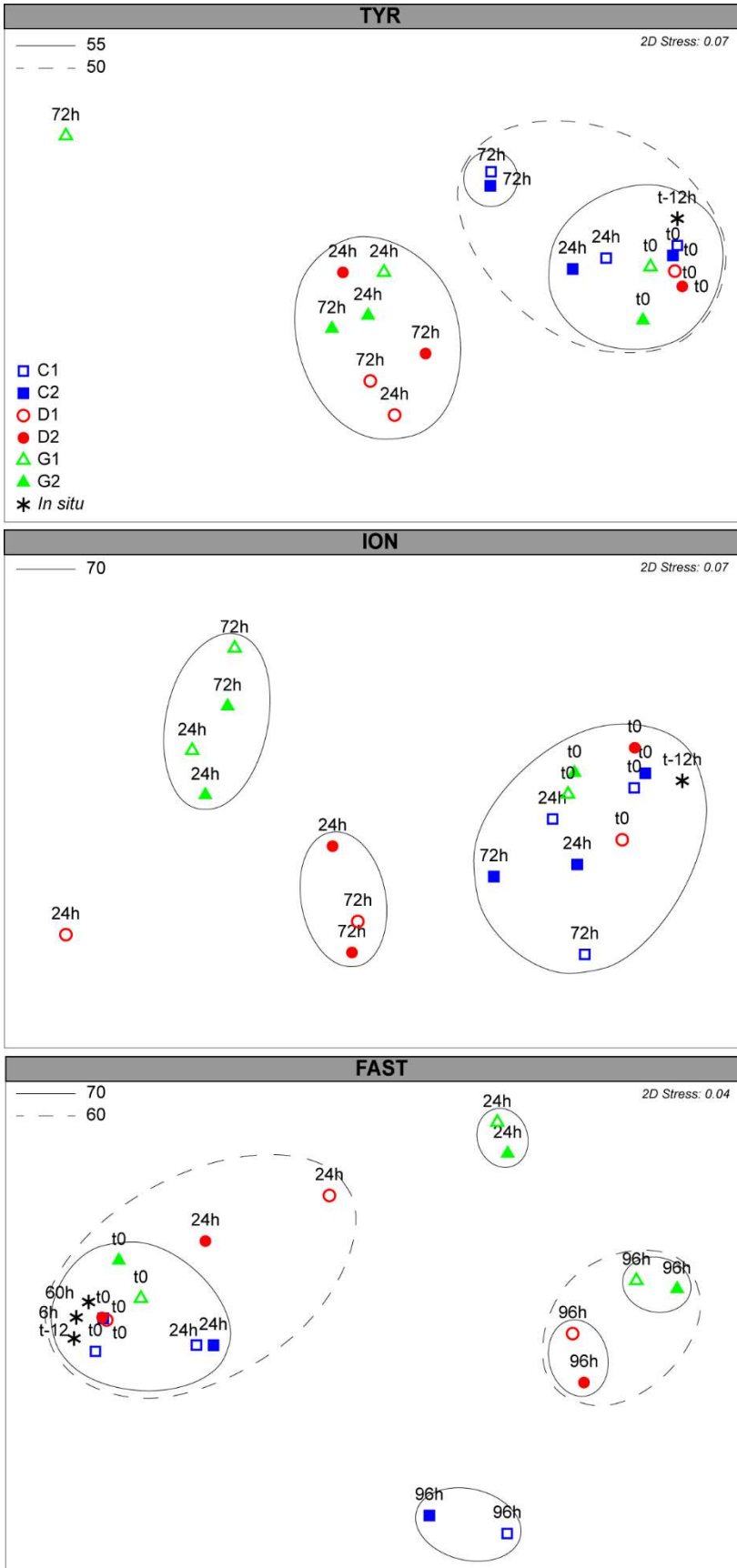


Figure 5.

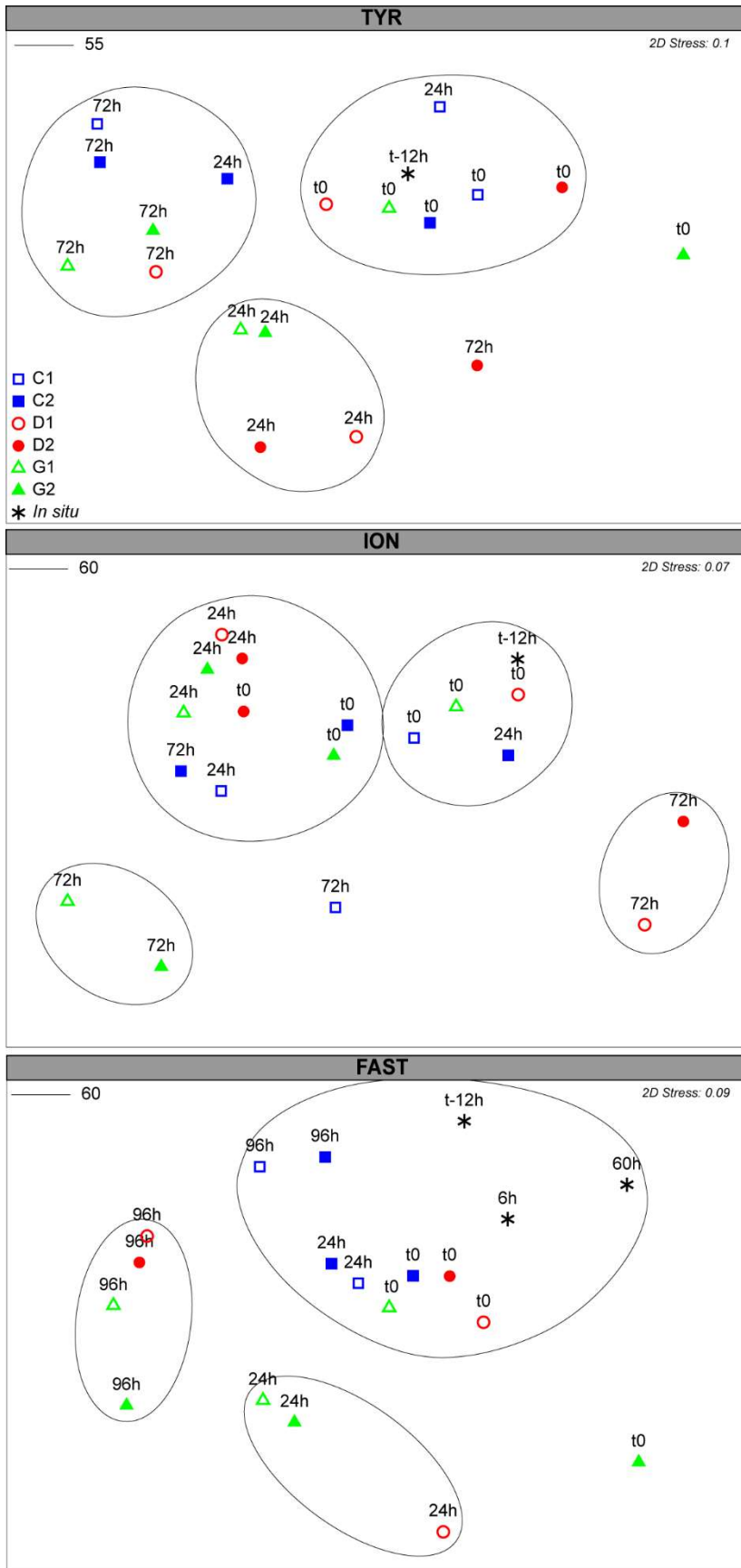


Figure 6.

